THE EVAPORATION FROM THREE DIFFERENT HIGH-LATITUDE SURFACES

by

ROBERT BRUCE STEWART, B.A., M.Sc.

A Thesis

Submitted to the School of Graduate Studies

in Partial Fulfilment of the Requirements

for the Degree

Doctor of Philosophy

McMaster University

May 1976

THE EVAPORATION FROM THREE DIFFERENT HIGH-LATITUDE SURFACES

DOCTOR OF PHILOSOPHY (1976)
(Geography)

McMASTER UNIVERSITY
Hamilton, Ontario

TITLE: The Evaporation from Three Different High-Latitude Surfaces

AUTHOR: Robert Bruce Stewart, B.A. (University of Windsor).
M.Sc. (McMaster University)

SUPERVISOR: Professor W. R. Rouse

NUMBER OF PAGES: ix, 94

ABSTRACT

This study examines the evaporation from a lichen-dominated upland ridge, a swamp and a shallow lake in the Hudson Bay lowlands evaluated by the energy-budget and equilibrium model approaches. Energy-budget calculations reveal that on average 54, 66 and 55 percent of the daily net radiation is utilized in the evaporative process over the ridge, swamp and lake surfaces respectively. For the ridge half-hourly and daily values of evaporation were approximated closely by equilibrium estimates, while for the other surfaces close approximation was achieved by the Priestley and Taylor (1972) model where the ratio of actual to equilibrium evaporation equals 1.26.

A simple model, expressed in terms of incoming solar radiation and the screen height air temperature, is developed for each surface from the comparison of actual to equilibrium evaporation. Tests of the models at different locations indicate that the actual evaporation can be estimated on a daily basis within 6 percent for dry upland and saturated lowland swamp surfaces, while for shallow lakes, the evaporation can be determined within 10 percent over periods of two weeks.

ACKNOWLEDGEMENTS

This study was supported by research grants from the National Research Council of Canada; the Department of Energy, Mines and Resources, Ottawa; and the National Geographic Society.

Special thanks is extended to my supervisor, Dr. W. R. Rouse, in appreciation for his invaluable guidance, assistance and support throughout this study. I wish to thank Dr. J. A. Davies for his assistance and constructive criticism in the course of preparing this thesis.

Further acknowledgement is extended to Dr. K. A. Kershaw, Mr. Peter Mills and Mr. Richard Bello for their help during the measurement program; to Miss Raymonde Thibeault for typing the final draft; and to Transair Midwest for allowing the use of their Hudson Bay field camp as a research site.

Finally, I especially wish to thank my wife, Patricia, for her untold support and perseverance during my academic endeavours.

TABLE OF CONTENTS

LIST OF FIGURES

LIST OF TABLES

LIST OF PLATES

CHAPTER I

INTRODUCTION AND PURPOSE

High latitude upland surfaces in Northern Canada present an unusual environment with respect to evaporation. For example, in the Hudson Bay lowlands Rouse and Kershaw (1971) found that for upland areas, dominated by spruce-lichen woodland vegetation, a strong biological control existed over the evaporative process. Although surface soil moisture content was at or near field capacity, the non-transpiring lichen vegetation strongly inhibited the flux of water vapour from the surface. A similar finding was noted by Stewart (1972) for a lichen-dominated raised beach ridge at East Pen Island. The latter's results suggested that evaporation from upland lichen surfaces could be estimated as a function of temperature and available radiant energy. Successful testing of his model over diverse lichen and burned surfaces subsequently showed that the resistance to evaporation by a variety of upland surfaces was similar. This implied that an evaporation model, based on the concept of equilibrium evaporation (Slayter and McIlroy, 1961), could be of general use in calculating the evaporation from upland surfaces which exhibit a uniform resistance to evaporation.

The aforementioned studies have been restricted to examining the evaporation from dry upland subarctic and tundra surfaces. To the author's knowledge, there have been no attempts to develop models of the

evaporative regimes of either lowland wet areas or shallow open water surfaces. Considering that in the Hudson Bay lowlands alone, an area of $3.0 \times 10^5 km^2$, 92 percent of the surface area is dominated by wet surface types (Rouse, 1973) and that many other high latitude areas are very wet, the importance of being able to accurately predict the evaporation from these surfaces is apparent.

Due to the inaccessibility of much of the subarctic and tundra region, and because of the large area involved, models for estimating the evaporation from both dry and saturated surfaces are desirable. One such model that lends itself to calculating the evaporation from both of these surface types was presented recently by Priestly and Taylor (1972). It expresses potential evaporation as a function of equilibrium evaporation estimates for diverse saturated surfaces. Recent developments, however, have also revealed that the same model form can be applied to estimating evaporation from non-saturated surfaces (Rouse and Stewart, 1972; McNaughton and Black, 1973). In either case, providing the ratio of actual to equilibrium evaporation remains constant, the evaporation can be estimated as a function of temperature and available radiant energy. In the Hudson Bay lowlands the presence of an abundant soil moisture supply, even for dry upland areas, suggests that various forms of the equilibrium model might be applicable to estimating the evaporation from several different surfaces. Furthermore, there is a lack of evaporation data involving different subarctic and tundra surfaces and, therefore, further research is warranted.

The purpose of this study is to evaluate simultaneously the evaporation from three different tundra surfaces. A lichen-dominated raised beach ridge, a swamp and a shallow lake in the Hudson Bay lowlands were investigated during July, 1972. Results of actual evaporation determined from the energy balance approach for each surface are presented. Equilibrium model estimates of evaporation are compared to energy balance measurements in order to test the hypothesis that surface control over the evaporative process is constant for a wide range of temperature. Extending from this, the hypothesis that evaporation from each surface can be accurately estimated as a function of temperature and incoming solar radiation is examined.

CHAPTER II

THEORY

1. The Energy Balance

From the principle of the conservation of energy the one-dimensional energy balance, in the absence of advective sensible and latent heat and neglecting photosynthesis and short term storage in the biomass, can be expressed as

$$Q^* - G = H + LE, \tag{1}$$

where Q^* is the net radiation, G is the heat flux across the earth-atmospheric interface, and H and LE are the sensible and latent heat fluxes respectively. L represents the latent heat of vapourization and E is the quantity of water evaporated. A complete list of symbols is given in Appendix A. Photosynthesis is neglected as an energy storer since, for slow growing lichens, mosses and sedges, it is several orders of magnitude less than the net radiation. In addition, the storage of heat energy in the plant biomass can be considered negligible since it has been shown to be small for hourly periods (Wilson, 1971) and tends to approach zero on a daily basis (King, 1961).

LE can be determined from equation (1) if the remaining components are known. However, since Q^* and G can be calculated or measured directly an indirect estimation of LE is usually obtained by partitioning the remaining energy between H and LE. This is accomplished using the Bowen Ratio, $\beta = H/LE$ (Bowen, 1926), such that equation (1) reduces to

$$LE = \frac{Q^* - G}{1 + \beta} . \tag{2}$$

The Bowen Ratio can be solved using one-dimensional mass transfer equations for H and LE

$$H = - \rho C_p K_H \bar{\Delta T}/\Delta z, \tag{3}$$

and

$$LE = - (\rho C_p/\gamma) K_W \bar{\Delta e}/\Delta z, \tag{4}$$

where γ is the psychrometric constant, ρ is the air density, C_p is the specific heat of air at constant pressure, K_H and K_W are the eddy diffusivities of heat and water vapour, $\bar{\Delta T}$ and $\bar{\Delta e}$ are the dry bulb temperature and vapour pressure gradients over a height increament Δz with the bar denoting a time average. Assuming $K_W = K_H$, which has been shown to be valid by Swinbank and Dyer (1967) and Dyer (1967), over a wide range of atmospheric stability:

$$\beta = H/LE = \gamma\bar{\bar{\Delta T}}/\bar{\bar{\Delta e}}, \tag{5}$$

and hence,

$$LE = \frac{Q^* - G}{1 + \gamma\Delta T/\Delta e}. \tag{6}$$

Further simplification of equation (6) can be accomplished by reformulating $\bar{\bar{\Delta e}}$ in terms of T and T_w, where T_w is the wet bulb temperature. The vapour pressure, (e), can be calculated utilizing the psychrometric equation:

$$e = e_s - \gamma(T - T_w), \tag{7}$$

where e_s is the saturation vapour pressure at the mean temperature ($T_M = (T + T_w)/2$). Over a finite height difference, (Δz), the vapour pressure can be computed as

$$\Delta e = (S + \gamma)\ \bar{\bar{\bar{\Delta T_w}}} - \gamma\bar{\bar{\Delta T}}, \tag{8}$$

where S is the slope of the saturation vapour pressure-temperature curve at the mean temperature between two levels of measurement. From equations (6) and (8)

$$LE = (Q^* - G)\left[1 - \left(\frac{\gamma}{S + \gamma}\right)\frac{\bar{\bar{\Delta T}}}{\bar{\bar{\bar{\Delta T_w}}}}\right]. \tag{9}$$

Dilley (1968) has shown that values of S, calculated from

$$S = \frac{25029}{(T_M + 237.3)^2} \exp\left[\frac{17.269\ T_M}{T_M + 237.3}\right] \qquad (10)$$

are accurate to within 0.1 of 1 percent of the values obtained from the Goff and Gratch (1946) formulae over the temperature range 0-50 C.

The determination of LE using equation (9) requires the measurement of Q* and G at the surface, and T and T_w for at least two levels. No knowledge of surface characteristics such as wetness, roughness or other parameters is required. It is essential, however, that the height-fetch ratio is adequate in order to avoid advectional effects. This insures that profile measurements of temperature and humidity are contained within the boundary layer, thereby, yielding representative values of the surface fluxes.

2. Equilibrium Evaporation

The equilibrium model is a special case of the combination approach to estimating the evaporative heat flux. Although the first general expression defining the combination method was presented by Penman (1948), similar formulations have been put forth by Slayter and McIlroy (1961) and Monteith (1965). The former's derivation is presented in the following discussion.

Slayter and McIlroy express the combination model for actual evaporation as

$$LE = \frac{S}{S + \gamma} (Q^* - G) + h(D_z - D_o), \tag{11}$$

where $D = T - T_w$ is the wet bulb depression, o and z are subscripts referring to the surface and some height above the surface, and h is a transfer coefficient that applies between o and z and varies with surface roughness and atmospheric stability. The method combines the energy balance approach with mass transfer theory. In this instance the sensible and latent heat fluxes were formulated as:

$$H = h\bar{\Delta}\bar{T}, \tag{12}$$

and

$$LE = (h/\gamma)\ \bar{\Delta}\bar{e}; \tag{13}$$

where $h = \int_o^z (dz/K_H)^{-1} = \rho C_p / r_a$, and r_a is the aerodynamic resistance.

Equations (12) and (13) can be redefined in terms of T_w and D with the use of equation (7), such that

$$LE = \frac{h}{\gamma} (S\bar{\Delta}\bar{T}_w - \gamma\bar{\Delta}\bar{D}) = \frac{hS}{\gamma}\ \bar{\Delta}\bar{T}_w - h\bar{\Delta}\bar{D}, \tag{14}$$

and

$$H = h(\bar{\Delta}\bar{T}_w + \bar{\Delta}\bar{D}), \tag{15}$$

where $T_w = T_{wa} - T_{wo}$ and $D = D_z - D_o$. Substituting equations (14) and (15) into equation (1), gives:

$$h\overline{\Delta T_w} = (Q^* - G)\ (1 + S/\gamma), \tag{16}$$

and utilizing equations (14) and (16), the latent heat flux reduces to the expression

$$LE = \frac{S}{S + \gamma}\ (Q^* - G) + \overline{h\Delta D}, \tag{17}$$

which is the combination model for actual evaporation.

The term, $\overline{h\Delta D}$, is the main factor which contributes to differences in LE between surfaces of different wetness having similar available radiant energy. For example, in the case where the air in proximity to a moist surface remains unsaturated, $D_o = 0$ and equation (17) reduces to the potential rate defined as

$$PLE = \frac{S}{S + \gamma}\ (Q^* - G) + \overline{hD_z}, \tag{18}$$

where PLE is potential evaporation. Slayter and McIlroy (1961) introduced the concept of equilibrium evapotranspiration by taking the limited case $D_z = D_o = 0$. In this instance equation (17) reduced to

$$LE = LE_{EQ} = \frac{S}{S + \gamma}\ (Q^* - G) \tag{19}$$

where, LE_{EQ} the equilibrium evaporation rate, is calculated simply as a function of temperature and available radiant energy.

The concept of LE_{EQ} is unique as it has been shown to apply in two opposing sets of environmental conditions. The first, occurs in a moist environment when both the surface and overlying air are saturated, such that, $D_z = D_o = 0$ (Slayter and McIlroy, 1961); Monteith, 1965; Fuchs and Tanner, 1968). Under these conditions LE_{EQ} has been interpreted as the lower limit of potential evaporation since equation (19) represents the minimum possible evaporation from a saturated surface. The second, has been found to occur in a moderately dry environment when neither the surface nor overlying air is saturated, such that, $D_o \approx D_z \neq 0$ (Denmead and McIlroy, 1970; Davies, 1972; Wilson and Rouse, 1972). In either case the evaporative flux is independent of windspeed, depending solely on temperature and available radiant energy.

More recently, the evaporation from various surfaces has been expressed as a function of the equilibrium rate. For example, Priestley and Taylor (1972) showed that potential evaporation on a daily basis was proportional to LE_{EQ} in the form

$$LE = \alpha \frac{S}{S + \gamma} (Q^* - G), \tag{20}$$

where $\alpha = LE/LE_{EQ}$. Using several sets of micrometeorological data from various surfaces with unlimited water supplies, they found an overall mean of $\alpha = 1.26$. Similar values have been shown to apply by Davies and Allen (1972) and Ferguson and Den Hertog (1975) for a moist rye-grass

surface and shallow lake, respectively. Other researchers have found that the form of equation (20) is a valid indicator of actual evaporation for surfaces where the evaporation differs from the potential rate. Rouse and Stewart (1972) found that α was relatively constant at 0.955 for diverse lichen and burned surfaces in the subarctic. McNaughton and Black (1973) found that $\alpha = 1.05$ for a relatively dry Douglas fir forest. In any case, provided α remains constant, the evaporation can be calculated more simply from a form of equation (20) than from equation (17) as there is no need to measure D_o, in the case of an unsaturated surface, or to specify a turbulent transfer mechanism.

CHAPTER III

SITE AND EXPERIMENTAL METHOD

1. Site

The study was conducted during July 1972, near the Hudson Bay coastline adjacent to East Pen Island in Northern Ontario (lat. 57°45'N., long. 88°45'W.). The location is shown in Figure 1. Observations were made over a predominantly flat raised beach ridge, a lowland swamp and a shallow lake, 15-20 km north of the treeline and approximately 2 km inland from the coast.

Vegetation in the vicinity of the site was typical of tundra vegetation, comprising lichens, mosses and lower order vascular plants on the beach ridges, with intermittent lakes and swamp between the ridges. The ridge surface, (Plate 1a), was covered by a lichen and lower order vascular plant vegetation varying from 30-70 mm in mat thickness. *Cetraria islandica*, *C. nivalis*, *C. cuculata*, and *Alectoria ochroleuca* were the main species of lichen, while the main lower order vascular plants were *Dryas integrifolia* and *Rhododeron lapponicum*. The vegetal cover was underlain by a sandy soil varying from fine to coarse sand.

The swamp, (Plate 1b), was dominated by grass and sedge vegetation with a few intermittent moss-covered hummocks. In addition to the vegetal cover, a surface layer of water varying from 10-30 mm was evident. The water and vegetal cover were in turn underlain by a thick frozen organic

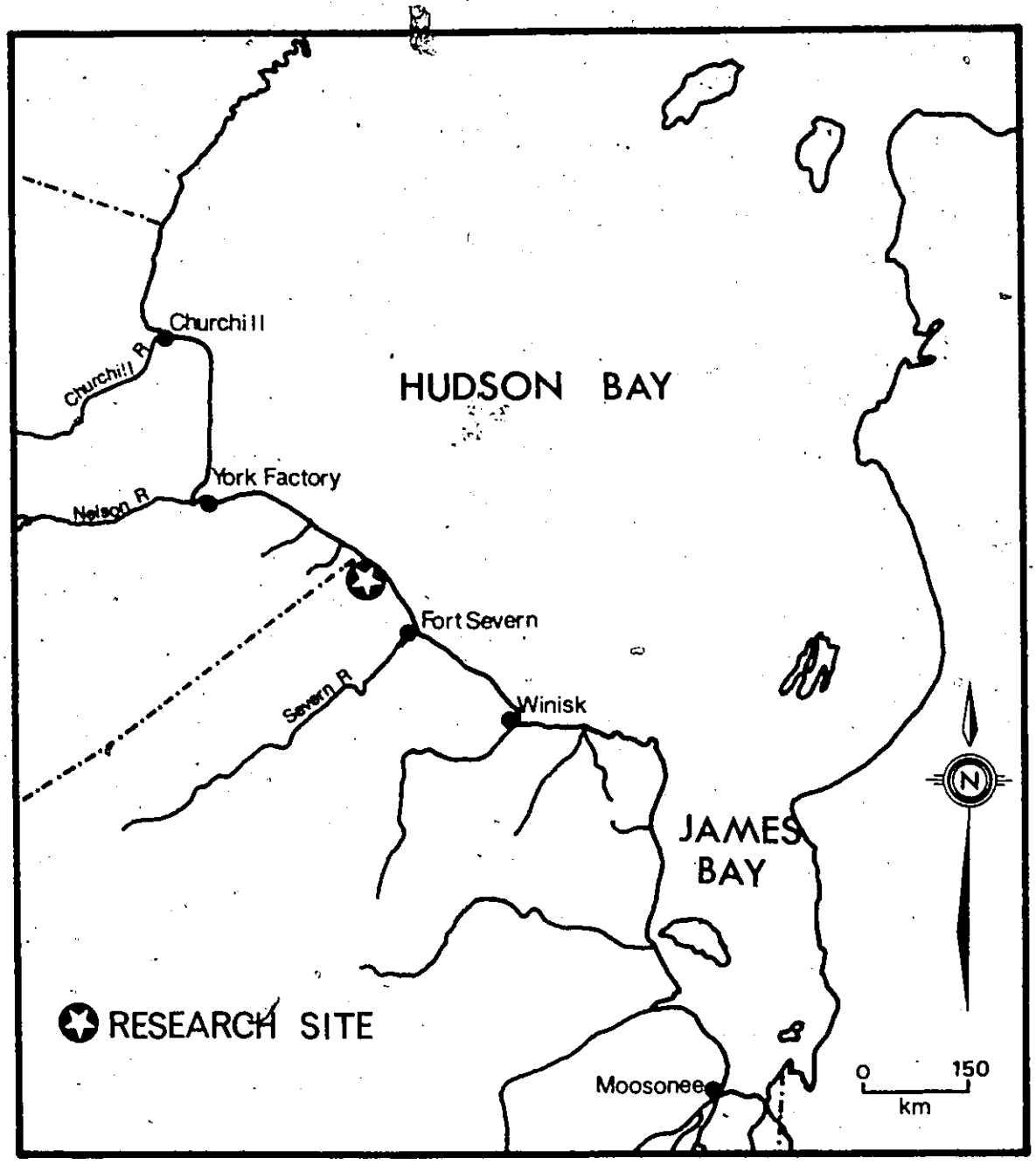

FIGURE 1: Location of Research Site

layer approximately 0.48 m in thickness which in turn covered a fine mixture of frozen sand and silt.

The lake surface, (Plate 1c), was roughly circular in shape with a diameter of about 400 m, a surface area of $10^5 m^2$ and an average depth of 0.59 m. A thick frozen mud layer formed the crust of the lake bottom. No surface drainage into or out of the lake was evident during the study.

2. Energy Balance Measurements

In order to evaluate the energy balance using equations (1) and (9) the measurements of net radiation, subsurface heat flow and the vertical dry and wet bulb temperature gradients above the surface are required.

a. Net Radiation

Net radiation was measured over each surface using Swissteco (Type S-1) net radiometers. These instruments, purged with the flow of dessicated air in order to equalize the convective loss from each of the thermopile surfaces and to prevent internal condensation, were mounted 1 m above the surface. Signals were continuously recorded by an Esterline-Angus 24 point recorder (Model E1124E) and integrated half-hourly totals determined by planimetering the pen traces. Q* values were then calculated using calibrations determined by the National Radiation Laboratory of the Atmospheric Environment Service. These are listed in Appendix B. Subsequent recalibration of each instrument after the experimental period showed no change in the calibration constants.

a) Ridge

b) Swamp

Plate 1 - View of the Ridge and Swamp Sites at Pen Island

c) Lake

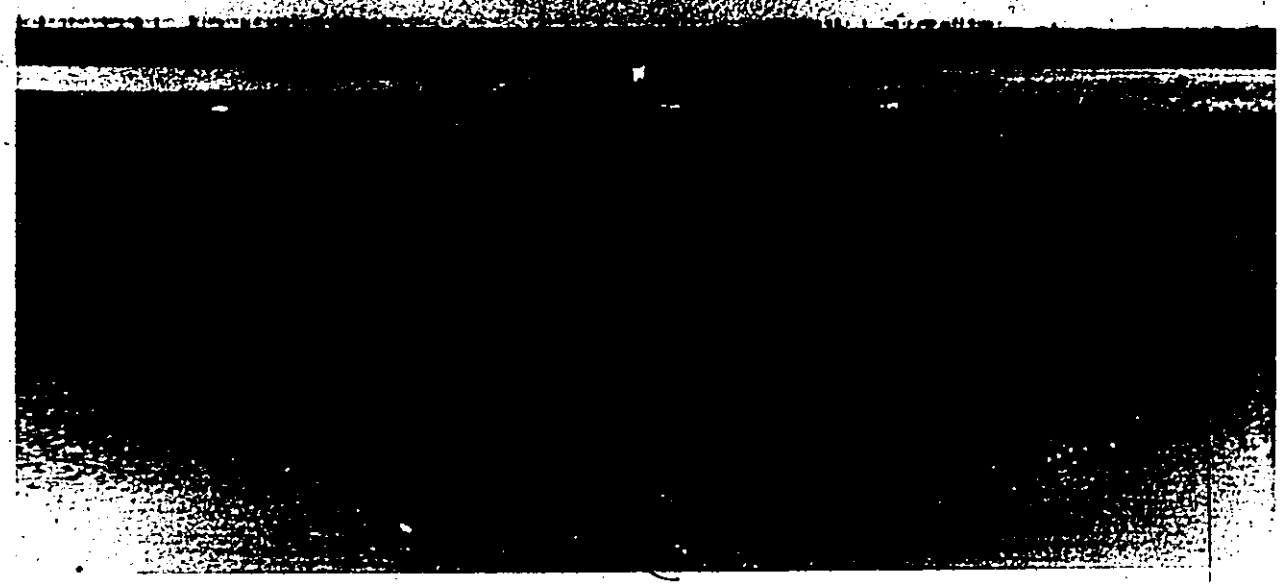

Plate 1 - View of the Lake Site at Pen Island

b. Subsurface Heat Flux

The subsurface heat flux, G, at the surface was calculated from the expression

$$G = G_z + C(\bar{\Delta T}_s/\Delta t)\ \Delta z, \tag{21}$$

where G_z is the heat flux measured at some depth below the surface, C is the heat capacity between the surface and depth z, $\bar{\Delta T}_s$ is the change in temperature between the surface and depth z over the time interval Δt, and Δz is the thickness of the soil layer from the surface to depth z. The soil heat flux at a depth of 50 mm was measured for the swamp and ridge surfaces with 3 soil heat flux plates (Middleton and Pty, Ltd.) connected in series. Changes in the mean temperature $\bar{\Delta T}_s$ in the layer 0-50 mm were monitored bi-hourly with ice-referenced thermocouples spaced at constant depth interval between the surface and soil heat flux plates.

The heat capacity of the soil was estimated from the equation given by De Vries (1963) in which

$$C = 0.46\ X_m + 0.60\ X_o + \theta, \tag{22}$$

where X_m, X_o and θ are the volumetric fractions of mineral matter, organic matter and water respectively. X_m and X_o were found to be 0.98 and 0.02 for the ridge and 0.15 and 0.85 for the swamp from "loss to ignition" treatments of surface samples. Using these values, equation (22) reduces to

$$C_R = 0.463 + \theta, \tag{23}$$

and

$$C_S = 0.579 + \theta \tag{24}$$

for the ridge and swamp respectively.

The average soil moisture content for the ridge was estimated twice a week with the use of a surface neutron probe (Nuclear Chicago 5901) while θ in the saturated swamp was constant at 0.26.

The heat flux into the lake was calculated as:

$$G_L = G_B + C_w \, (\overline{\overline{\Delta T_L}}/\Delta t) \, \bar{d} \tag{25a}$$

where G_B is the heat flux through the bottom of the lake, C_w is the heat capacity of water, $\overline{\overline{\Delta T_L}}$ is the average temperature of the lake from the surface to the lake bottom and $\bar{d}$ is the average depth of the lake.

The heat flux through the bottom of the lake was estimated from the rate of melting of the frozen mud that took place during the experimental period. At the beginning of the study the frost line was 50 mm below the surface of the lake bottom while at the end it was .36 m below the initially observed level. Assuming the melt layer was at 0 C, with a 50% volumetric water content and only the heat of fusion involed, G_B was estimated at approximately 0.039 MJ m^{-2} hr^{-1}.

With the heat capacity of water equivalent to 0.04184 MJ m^{-2} C^{-1}, and an average depth of 0.59 m, obtained from the average of 75 depth

soundings, the heat flux into the lake was computed for half-hourly intervals as:

$$G_L = 0.09146 + 2.46856\ \overline{\overline{\Delta T}}_L \qquad (25b)$$

where G_L is in MJ m^{-2}. Changes in the average lake temperatures were obtained by using a number of 5-junction thermopiles in series spaced at constant depth intervals between the surface and the lake bottom. The temperature was recorded continuously on an Esterline-Angus 24-point recorder (Model E1124E). Values extracted from the strip chart record every half hour were utilized in determining $\overline{\overline{\Delta T}}_L$.

c. Temperature and Humidity

Wet and dry bulb air temperatures over each of the surfaces were measured with 5-junction thermopiles similar to those described by Rouse and Kershaw (1971) and Wilson (1971). Junctions, enclosed in an aluminum sleeve filled with polyester resin, were constructed from standard 36 gauge copper constantan wire. Exposed junctions at the ends of the steel shafts were inserted in polyvinyl chloride (PVC) tubing and the juncture sealed with epoxy resin.

The temperature sensors were calibrated against a platinum resistance thermometer (Rosemount Eng. Co.) over the temperature range 0 to 30 C. Reversal of the hot and cold thermopile junctions during the calibration showed that the sensor sensitivity remained symmetrical. The calibration equation, constant for all sensors, is

$$\Delta T = -0.018 + 5.268\ V + 0.047\ V^2, \qquad (26)$$

where ΔT is the temperature difference between the hot and cold junctions of the thermopile and V is the electrical output of the thermopile in millivolts. Recalibration of the sensors after the experimental period showed no change in the calibration expressed in equation (26).

Wet and dry bulb air temperatures were measured over each surface using 3-level masts illustrated in Plate 2. The sensors were placed at heights of .25, .50 and .75 m above the surface and were contained within double-walled, aspirated radiation shields in order to minimize radiation and other local heating errors. Each sensor was referenced to an ice bath. Wet bulb sensors were enclosed in a tight-fitting muslin wick which extended from the base of the sensor through plastic tubing to a water reservoir. Water feed rates to the thermopile were readily adjusted by varying the height of the reservoir relative to the sensor head.

Height-fetch limitations differed for each of the sites. The ridge surface had an unlimited height-fetch ratio in the north and south directions, while in the east and west directions the ratio was approximately 1:200. The swamp had an unlimited fetch in the north and south directions. However, in the east-west direction the swamp was approximately 250 m wide. Since the weather conditions observed with easterly winds had previously been associated with storm conditions (Stewart, 1972) the temperature and humidity mast was located approximately 175 m from the western boundary. This maximized the height-fetch ratio for wind directions varying from the south through west to north sectors.

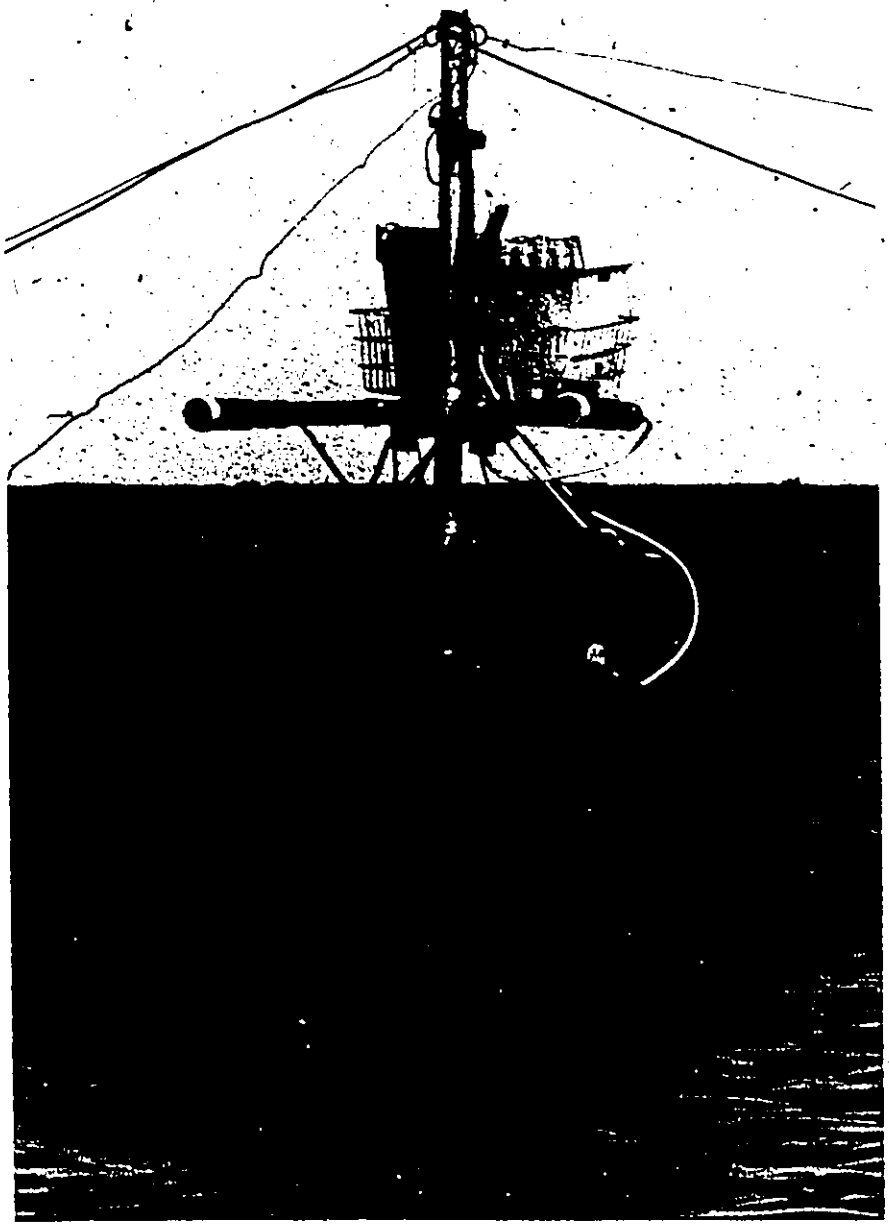

Plate 2 - Three-Level Bowen Ratio Mast

The installation in the lake was located as near its center as possible giving a height-fetch ratio in all directions of approximately 1:200. The fetch from the east direction, however, was unusable due to the obstructions created by the poles used to keep the various signal and power cables to the instrument towers above water. Thus, for the swamp and lake, all temperature and humidity data with easterly wind conditions were discarded. For all other wind directions the temperatures, monitored at heights of .25, .50 and .75 m above the surface, were well within the atmospheric boundary layer.

Temperature signals from the ridge and swamp were stepped through a double 6-channel stepping switch and recorded on a 2-pen Rickidenki (Model B-14) recorder. Temperature signals from the lake were stepped through a double 3-channel stepping switch and recorded on a 2-pen Honeywell (Model 194) recorder. The stepping switches allowed the wet and dry bulb temperatures at a given level, over each surface, to be recorded simultaneously. The speed of the stepping switches was adjusted to give 14 signals per half hour for each sensor. The millivolt signals were converted to temperatures and half hourly average values computed.

Values of the evaporative and sensible heat fluxes were computed from data for the height pairs .25 - .50 m, .50 - .75 m and .25 - .75 m over each surface. Three level evaluation ensured that values could still be determined in the event of sensor failure at one level.

An error analysis, which is presented in Appendix C, was performed on the temperature and humidity data to assess the accuracy of calculated vapour pressures. These were then combined with assigned maximum potential errors for Q^* and G in evaluating the error in LE estimates. The

results show that when temperature and humidity differences are large the evaporative estimates are accurate to within ± 7-12 percent for all three surfaces. This is probably an inadvertent underestimate, however, due to additional sources of error, including radiational heating of the sensors and errors involved in the extraction of data from the chart recordings which could not be assessed and are not included in the error calculations.

3. Measurements and Calculations for the Equilibrium Model

The same measurements made for the energy balance were utilized in evaluating the equilibrium evaporation for each surface as developed in equation (19).

In addition to measurements required for evaluation of the energy-budget and equilibrium evaporation, wind speed and direction, precipitation, and screen height air temperatures were recorded. The general meteorological data was monitored for 55 days between June 25 and August 14.

CHAPTER IV

ENERGY BALANCE AND EQUILIBRIUM EVAPORATION

1. Energy Balance

Daily variations of the energy balance components are shown in Figure 2. Component values are expressed as a percentage of net radiation. Although the distribution of Q* into the component fluxes H, LE and G differs for each surface, the patterns are similar since evaporation is the dominant component over each. For the lake, however, exceptions are evident with heat storage dominating on three days, July 4, 7 and 21. On average the ratio of LE/Q*, H/Q* and G/Q* was 54:37:9 for the ridge, whereas for the swamp, it was 66:26:8. LE for the lake was the largest component utilizing approximately 55 percent of Q*. The heat storage component was large accounting for 25 percent of Q* while H comprised 20 percent. Q* for the ridge and swamp averaged 82 and 72 percent of the lake value respectively.

Average values of the Bowen Ratio and air temperature for daylight periods are shown in Figure 3. Bowen ratios for the swamp and lake surface over the same time intervals show little difference, having mean values of .380 and .365 respectively. Values ranged between .194 and .568 for the swamp and between .083 and .634 for the lake. β values for the ridge differed from those for the lake and swamp with an average of .698 and a range from .992 on July 3 to .317 on July 10. Comparison

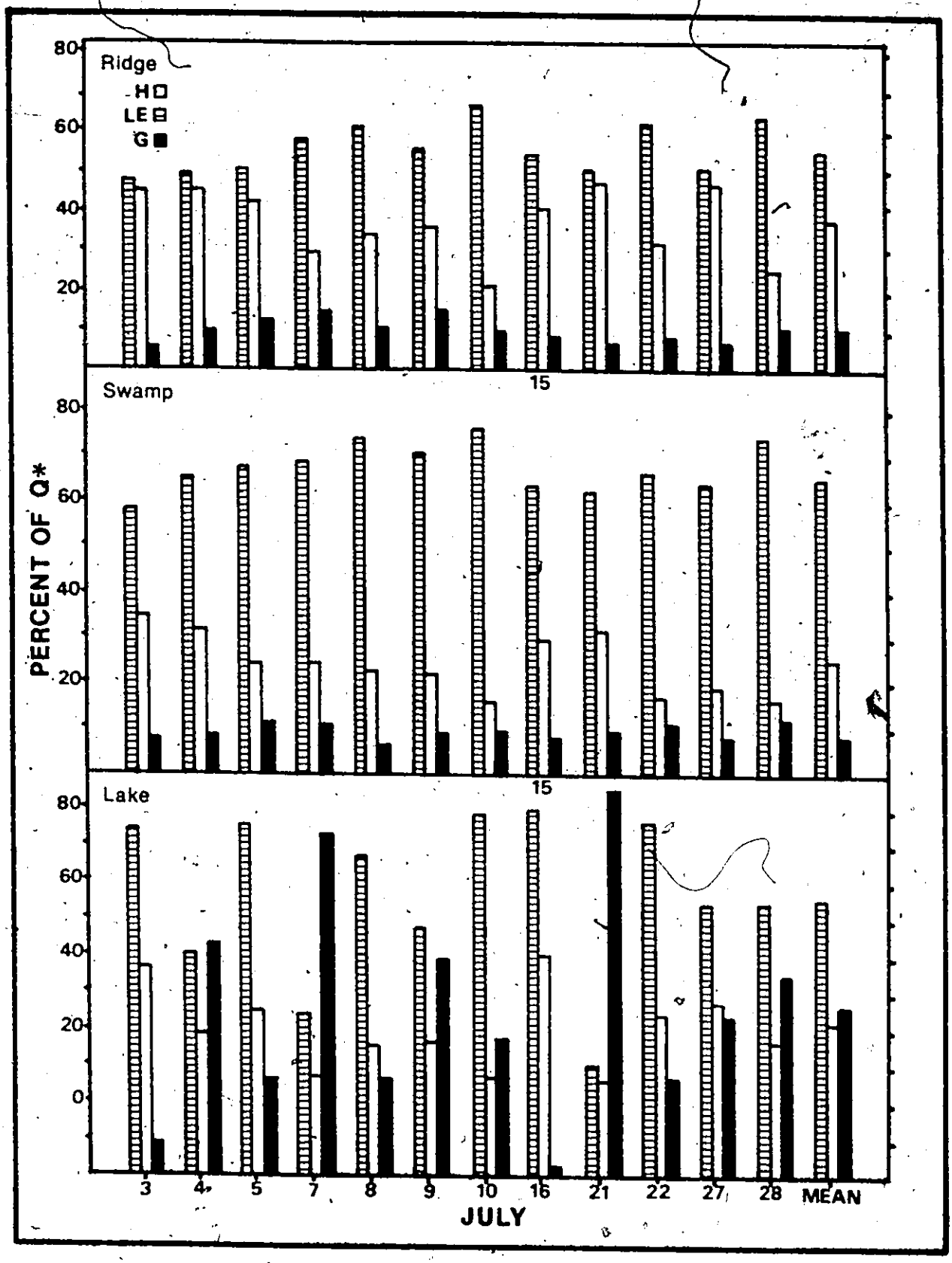

FIGURE 2: Daily Patterns in the Energy Balance Components for the Ridge, Swamp and Lake Surfaces

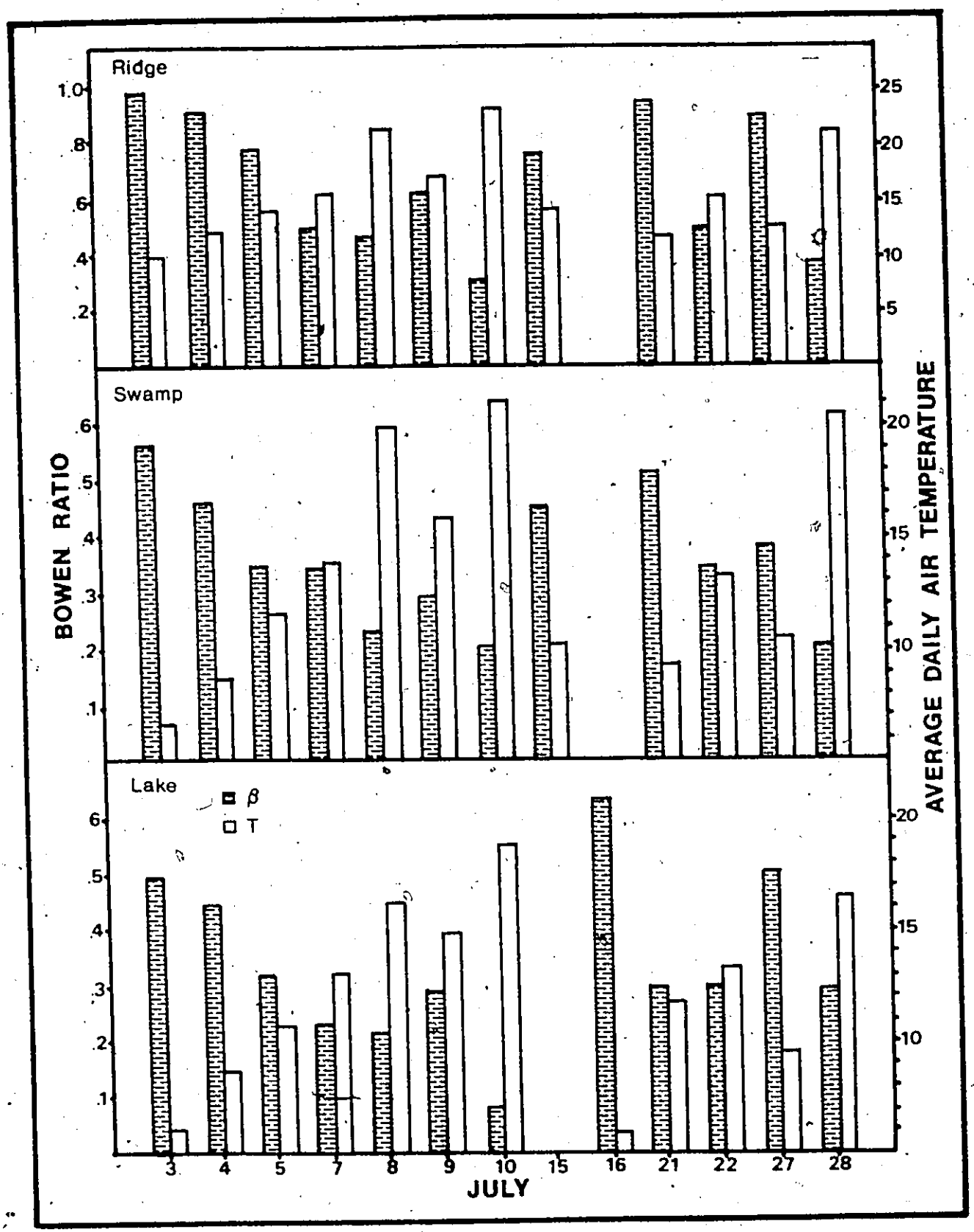

FIGURE 3: Daily Patterns of the Bowen Ratio and the Average Air Temperature

of Figures 2 and 3 show the variation of β with temperature and resultant changes in the energy balance components. In general, β shows a marked inverse relationship with air temperature over each surface (Figure 4). The equations for the lines plotted in Figure 4 were determined from equations (1) and (20). A value of 1.00 was utilized for α in the case of the ridge while for the swamp and lake, the Priestley and Taylor value of 1.26 was used. For each surface the temperature was weighted to the evaporation for comparative purposes with β, such that:

$$T_{WT} = \sum_{i=1}^{n} \frac{LE_i}{LE_{TOT}} T_i, \qquad (27)$$

where T_{WT} is the weighted average daily temperature, LE_i is the evaporation for half hour i, LE_{TOT} is the total evaporation for the day, n is the total number of half hours in the daily period and T is the temperature at time i. The relatively good agreement between computed and experimentally determined β values for each surface is evident. The importance of this fact is discussed in a later section.

Variations in β are accentuated in the energy balance components of the lake where the influence of the air temperature on the actual lake temperatures is apparent. A comparison of mean air temperatures with mean lake water temperatures (Figure 5, after Rouse (1973)) shows that lake temperature changes occur as rapidly as the day-to-day changes in atmospheric temperature. The effects of these changes are emphasized in the highly fluctuating changes in heat storage content of the lake during daylight hours. Much of the energy utilized in warming the lake is later released as evaporation during the night when the lake is

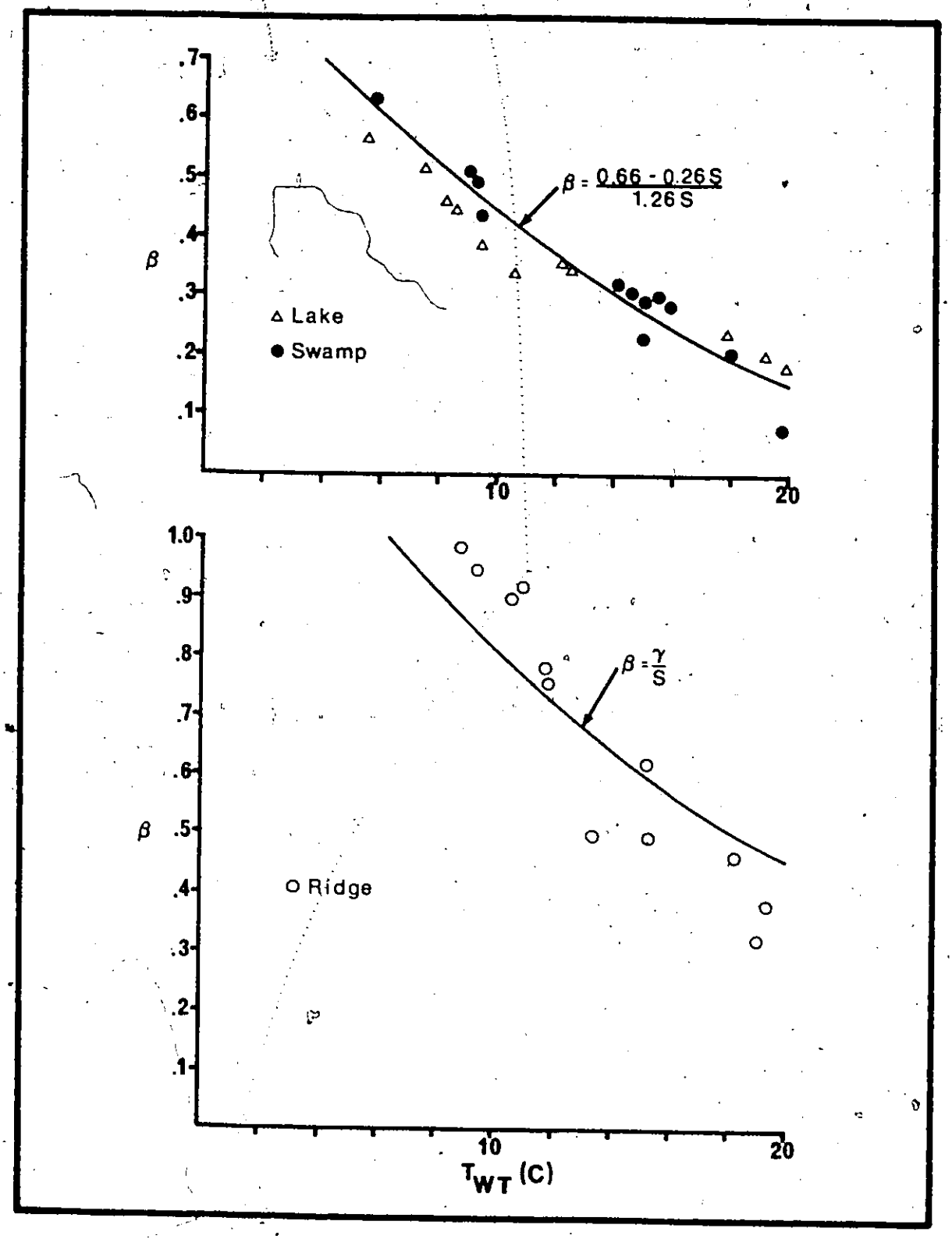

FIGURE 4: Comparison of Average Daily Bowen Ratios with Daily Weighted Average Air Temperatures for the Swamp, Lake and Ridge Surfaces

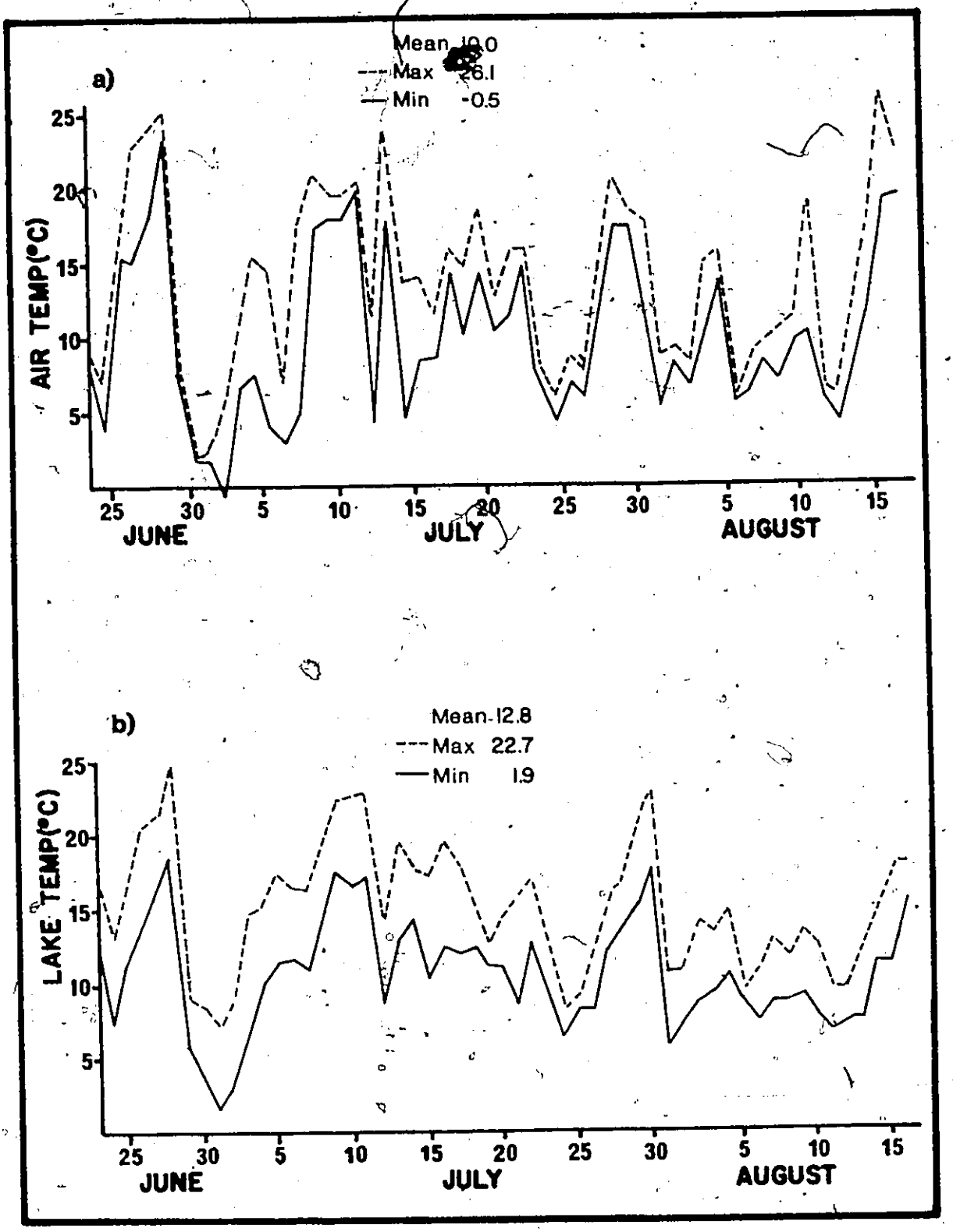

FIGURE 5: Seasonal Variation in the Daily Maximum and Minimum Air Temperatures and Lake Water Temperatures

cooling. This is seen in Figure 6 which compares the hourly variation in β and temperature during daylight periods with variations at night. The line through the latter, in Figure 6, represents the average daylight relationship of β to T for the lake, while, the point plots represent the night-time hourly values for July 3-4, 5-6 and 27-28. The comparison shows that the percentage distribution of nocturnal and daylight available radiant energy into H and LE is constant.

Comparison of the variations in daily β for the three surfaces shows that, although there is a difference in the magnitude of β, the curves tend to parallel one another. The latter feature is attributed to temperature which operates similarly over each surface, while the former is the result of differences in surface type and any surface moisture restrictions. The small magnitude and similarity of the Bowen ratio values for the lake and swamp indicate the absence of any surface control over evaporation. On the other hand, high values for the ridge indicate a strong surface control. Precipitation and surface soil moisture measurements (Table 1) shows that soil moisture varied little over the ridge. During the main experimental period, July 3-10, no rainfall was recorded while only 4 mm was received in the preceeding two weeks. At the same time, surface soil moisture content remained constant during the entire month of July at about 12 percent by volume, which, as shown by Rouse and Kershaw (1973), represents field capacity at the 10 kpa. matrix suction level. The precipitation data, Table 1, further support this view since even after substantial rainfalls on July 11, 15 and 17, the surface moisture content remained constant. Hence, the moisture utilized in evaporation from the ridge must have come from the

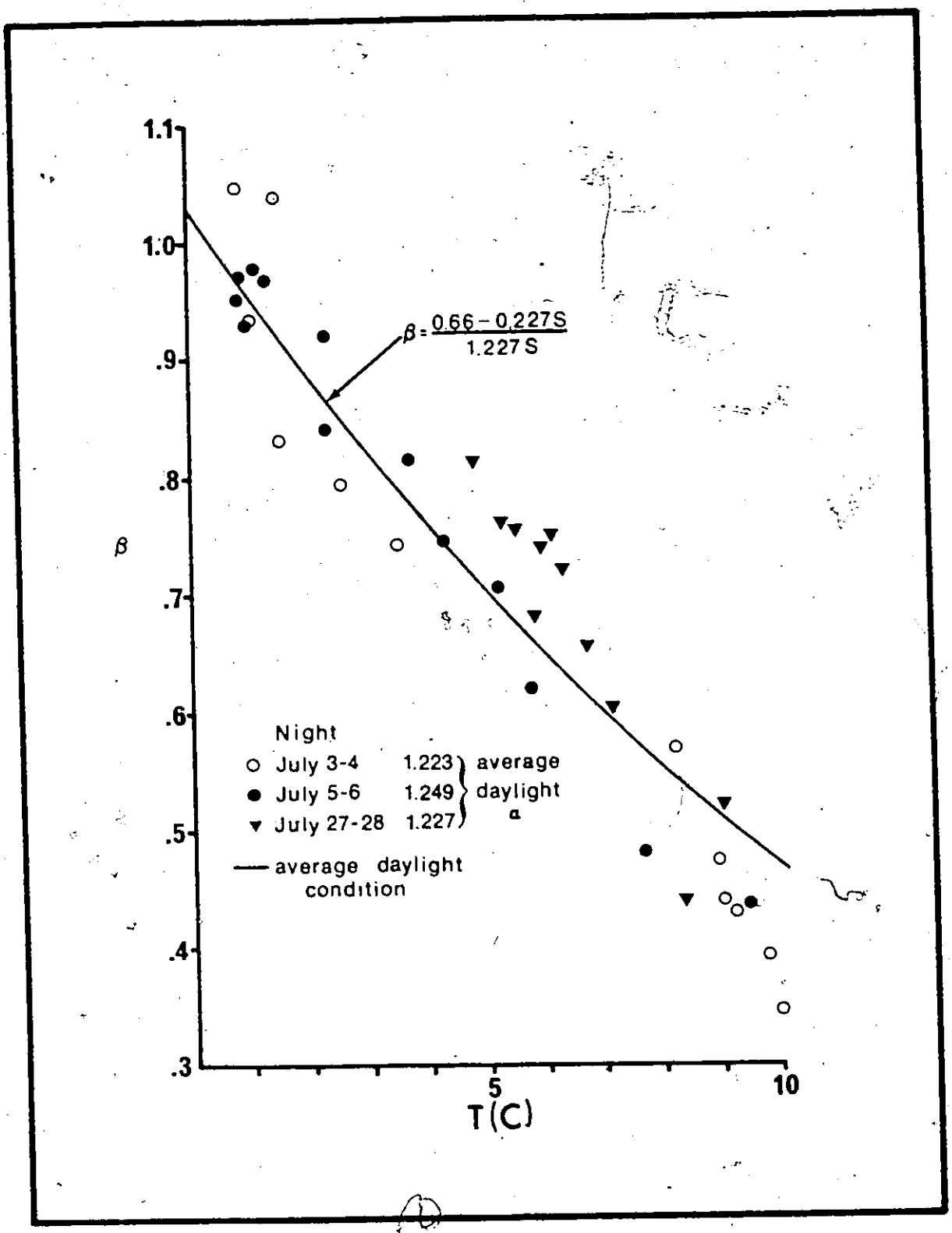

FIGURE 6: Comparison of Hourly Night-Time Bowen Ratios and Temperature to Average Daylight Conditions

TABLE 1

DAILY METEOROLOGICAL AND SURFACE SOIL MOISTURE DATA

FOR THE MONTH OF JULY

DATE		1	2	3	4	5	6	7	8	9	10	11	12	13	14	15	16
Temperature (°C)	Max.	3.2	6.0	10.6	15.4	15.5	6.5	18.2	23.2	20.5	23.2	24.4	15.0	23.9	15.7	14.2	12.0
	Min.	0.2	-1.5	-0.5	0.8	2.3	0.8	0.2	11.5	8.2	10.8	5.5	3.5	9.0	4.2	3.2	5.0
Wind Direction		NNE	NNE	N	NNW	NW	E	NW	W	SW	SW	SW	NW	W	N	NW	E
Precipitation (mm)												35.6				12.7	
Surface Soil Moisture (% vol.)	Ridge*	0.12						0.12							0.12		

DATE		17	18	19	20	21	22	23	24	25	26	27	28	29	30	31
Temperature (°C)	Max.	17.7	14.4	18.9	12.2	15.8	15.9	7.9	7.2	8.7	9.8	13.8	26.0	21.9	20.7	9.5
	Min.	4.1	5.7	5.1	5.1	5.1	7.1	4.9	4.1	5.0	5.0	6.6	6.1	13.5	5.1	4.1
Wind Direction		W	W	W	N	NW	NW	E	N	NNW	NNE	E	S	SSW	WNW	NNW
Precipitation (mm)		21.6			14.0									12.7	19.8	
Surface Soil Moisture (% vol.)	Ridge*			0.12									0.12			

*(After Mills, 1973)

available soil moisture. These findings, in conjunction with those of Kershaw and Rouse (1971) and Rouse and Kershaw (1973), who noted the seemingly large and unvarying soil moisture conditions under various lichen and burned surfaces, suggest that the soil moisture is virtually non-limiting to evaporation even for the supposedly drier surfaces in the Hudson Bay lowlands.

The similar temporal trends in the Bowen ratios for the ridge, swamp and lake indicate that the evaporation for each may be dictated by a constant surface control. This may create the differences in the average magnitude of β between the various surfaces, while temperature could be the main control underlying the day-to-day variation. To test this hypothesis, the evaporation estimates obtained by the energy balance approach were compared with equilibrium model estimates of evaporation, the latter being a method that computes LE solely as a function of temperature and available radiant energy.

2. Comparison of Actual to Equilibrium Evaporation

As previously shown in equation (20), the evaporation for a surface over any time period can be expressed as a function of equilibrium evaporation. The α parameter expresses the ratio of actual LE to equilibrium evaporation, LE/LE_{EQ}, where in most instances $0 \leq \alpha \leq 1.26$, although values greater than 1.26 are possible. The lower limit represents the case of no evaporation while the upper limit is the value that Priestley and Taylor (1972) consider to represent potential evaporation.

In examining the supposition that the evaporation for each surface is predominantly a response to the overlying air temperature and available

radiant energy, a number of things can be looked for in comparing LE to LE_{EQ}. First, the magnitude of α is inversely related to the surface resistance. Second, the day-to-day variations in the magnitude of α will indicate the stability of the surface control over the evaporative process. For example, combining equation (20) with Monteith's expression for actual evaporation in which

$$LE = \frac{S(Q^* - G) + \rho C_p \delta e / r_a}{S + \gamma + \gamma r_s / r_a} \tag{28}$$

yields the relationship

$$\alpha = \frac{1/\gamma + r_I / S r_a}{1/\gamma + \left(\frac{r_s / r_a}{S + \gamma} \right)}, \tag{29}$$

where r_s represents the stomatal resistance for a transpiring vegetation surface or surface resistance in the case of a non-transpiring surface and, r_I is the climatological resistance (Thom, 1972) or isothermal resistance (Monteith, 1965). r_I is a property of the atmosphere with the dimensions of a diffusive resistance equated to $\rho C_p \delta e / (Q^* - G)$, where, δe is the saturation vapour pressure deficit. It is apparent from equation (29) that α, and hence the evaporation rate, depends on the relative values of r_s, r_a and r_I. Thus, if α remains relatively constant the values of the various resistances should be, for the most part, constant. This is interpreted to exemplify stability in surface control over the evaporative process. Conversely, if α fluctuates erratically, one or more of the resistances must change substantially. This shows

instability in the surface's ability to control the evaporative process.

It is hypothesized that if there are no soil moisture restrictions, α should remain virtually constant. From this it follows that, if α is known, variations in the evaporative flux can be calculated solely from temperature and available energy. This hypothesis was tested for the ridge, swamp and lake surfaces by comparing both half-hourly and daily totals of equilibrium estimates of evaporation with those determined from the energy budget.

For the ridge and swamp surfaces, the half-hourly and daily totals refer to daylight totals which during the study averaged about 18 hours in length. For the lake the half-hourly and daily totals refer to the full diurnal period. Comparison of half-hourly values of actual LE with LE_{EQ} for each surface is shown in Figure 7. Results of a linear regression analysis is shown in Table 2. The good agreement in the relationships between half-hourly values of LE and LE_{EQ} is evident. Comparisons of daily totals of LE to the LE_{EQ} are shown in Figure 8. Support for the relationships is emphasized by the high correlation coefficients and low standard errors. For the ridge a line with $\alpha = 1.00$ fits the data quite well, while for the swamp and lake, a line representing $\alpha = 1.26$ fits the data. Since the lake and swamp surfaces represent potential evaporation conditions, further support is given to the Priestley and Taylor α value of 1.26.

From the comparison of LE with LE_{EQ}, and the resultant knowledge of α, the various resistances for each surface can be calculated. From this, variations in the resistances and resultant changes in α can be ascertained. With substitution of $\alpha = 1.00$, the surface resistance can be

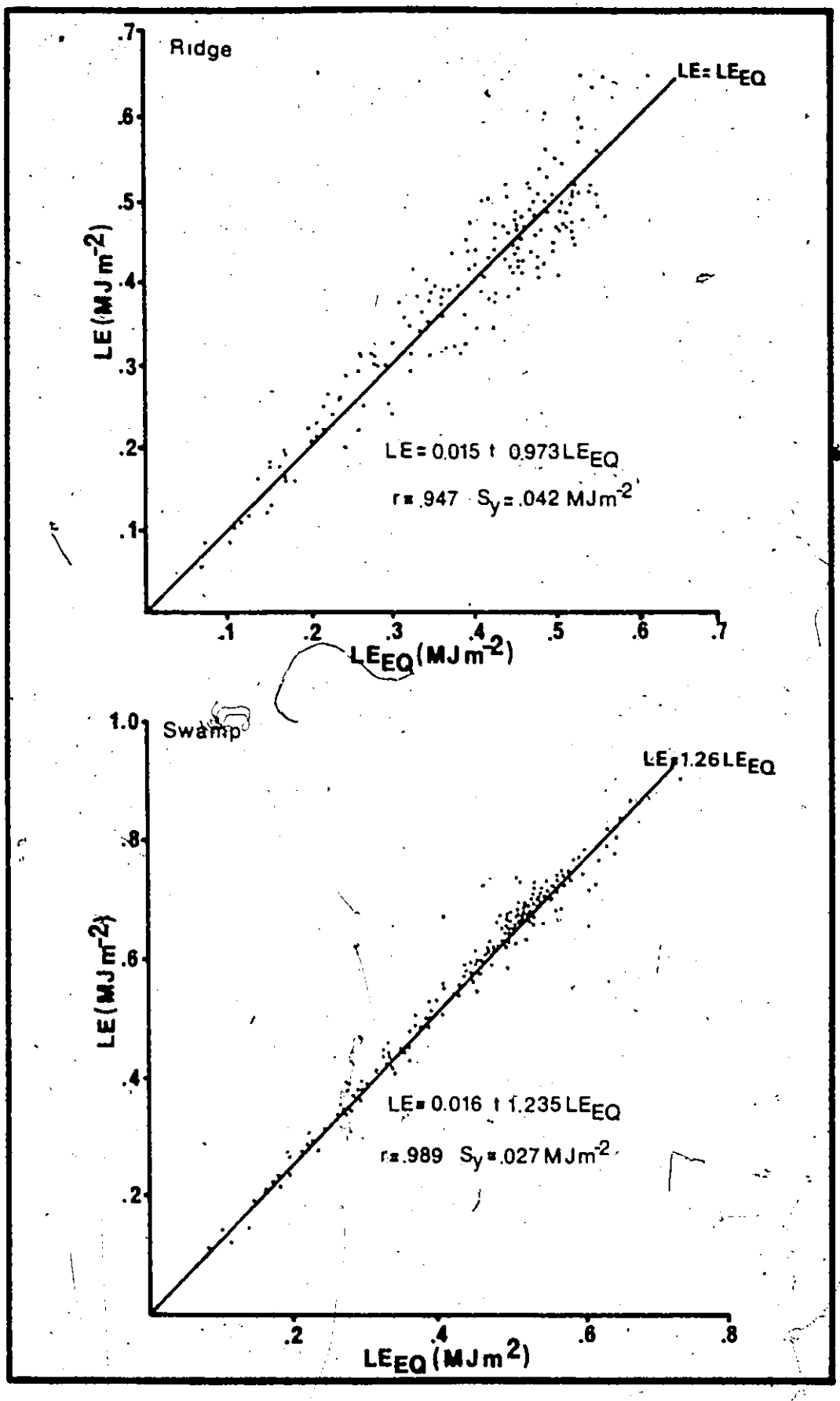

FIGURE 7: Comparison of Half-Hourly LE to LE_{EQ} for the Ridge and Swamp

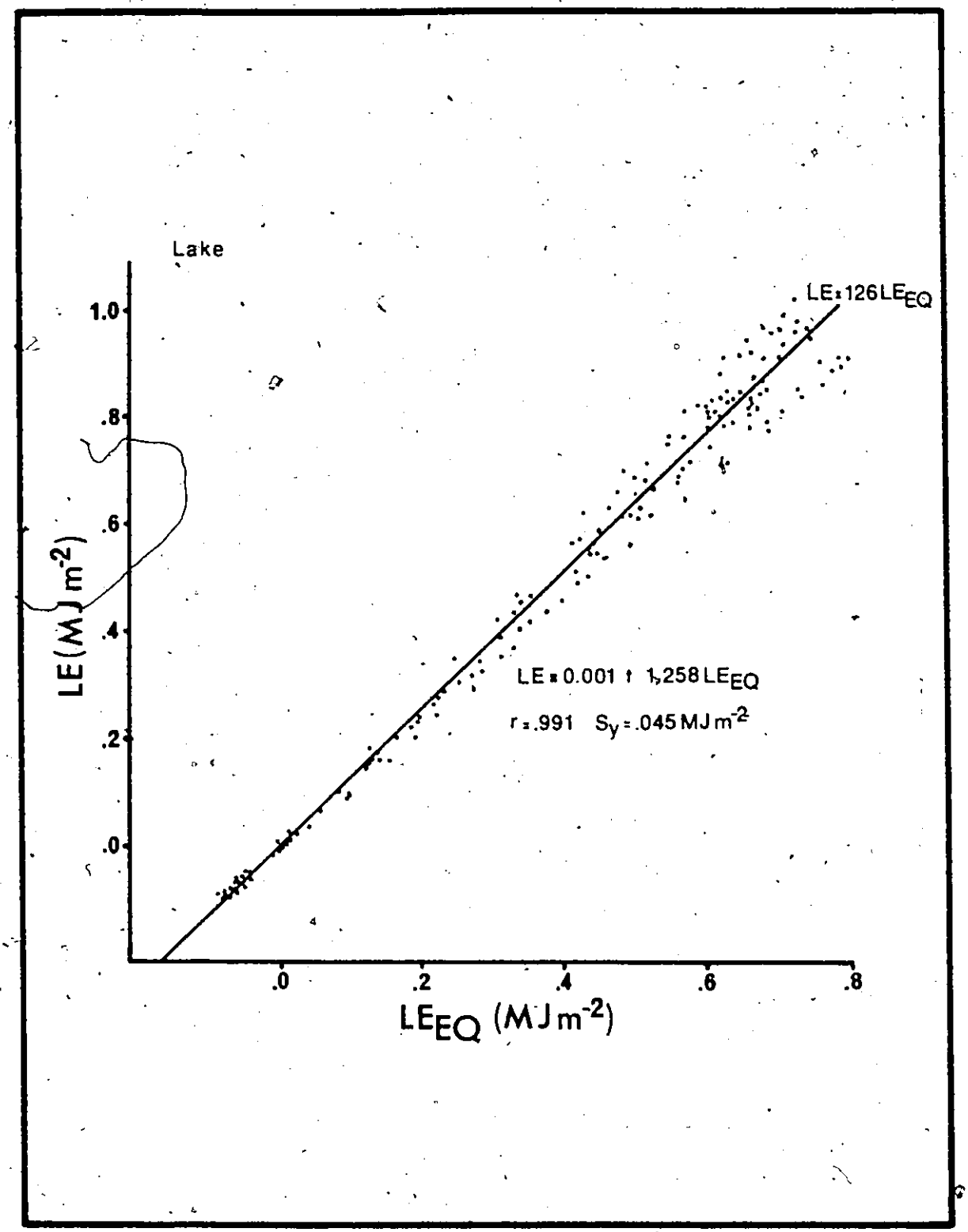

FIGURE 7: Comparison of Half-Hourly LE to LE_{EQ} for the Lake

TABLE 2

REGRESSION AND CORRELATION CONSTANTS FOR RELATIONSHIPS BETWEEN

LE and LE_{EQ} OF THE FORM LE = a't bLE_{EQ}

SURFACE	UNITS	NO. OF VALUES	Y-INTERCEPT	SLOPE	COEFFICIENT OF CORRELATION (r)	STANDARD ERROR OF THE ESTIMATE AT THE MEAN (Sy)
Ridge	MJ m^{-2} half hr^{-1}	177	0.015	0.973	0.950	0.042
Ridge	MJ m^{-2} day^{-1}	12	1.262 0.017	0.806 0.956	0.945 0.976	0.328
Swamp	MJ m^{-2} half hr^{-1}	177	0.016	1.235	0.989	0.027
Swamp	MJ m^{-2} day^{-1}	12	-0.195	1.303	0.996	0.177
Lake	MJ m^{-2} half hr^{-1}	196	0.001	1.258	0.991	0.045
Lake	MJ m^{-2} day^{-1}	12	0.201	1.227	0.999	0.184

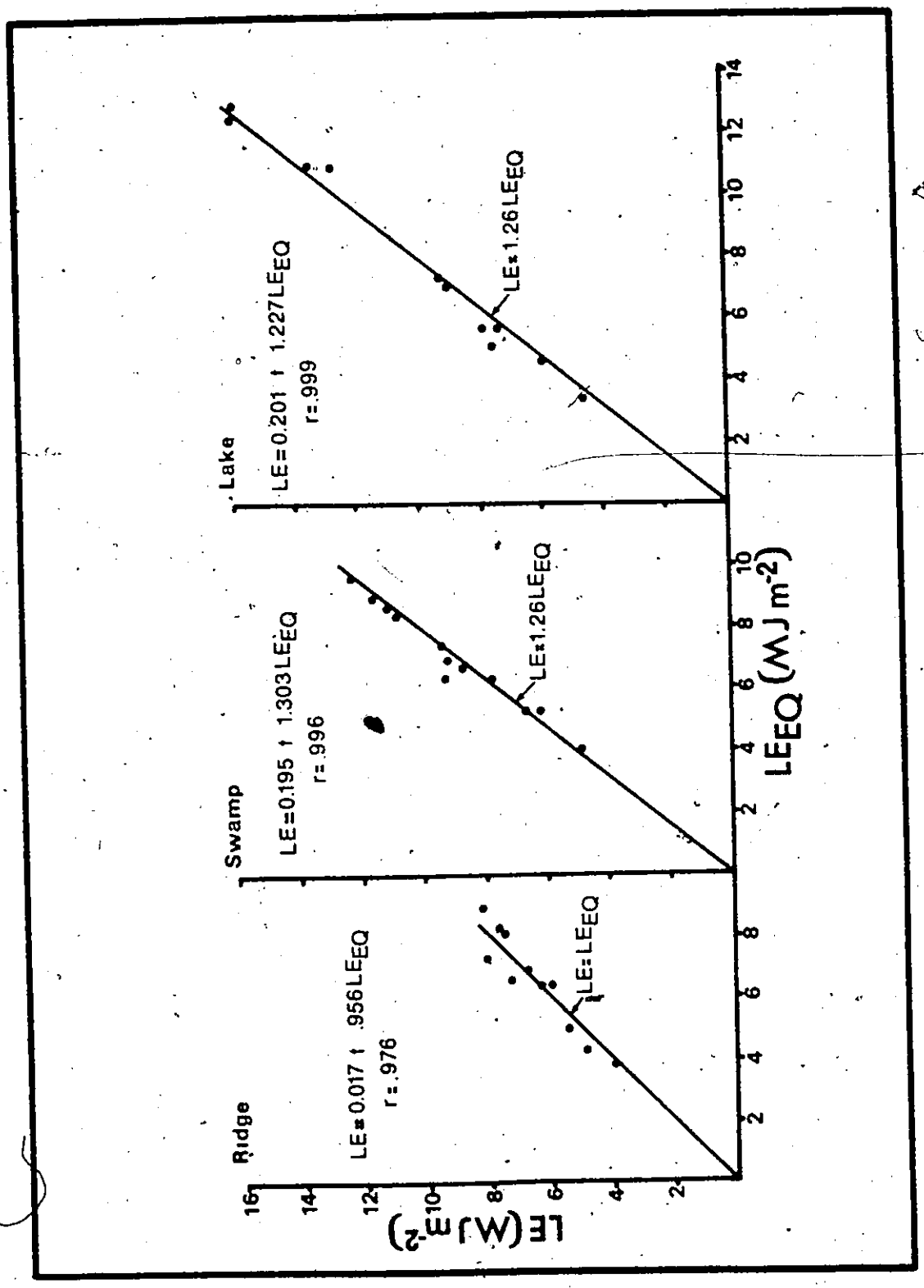

FIGURE 8: Comparison of Daily Totals of LE to LE_{EQ} for the Ridge, Swamp and Lake Surfaces

computed from equations (29) as

$$r_s = \frac{S + \gamma}{S} r_I, \tag{30}$$

where the evaporation rate is independent of r_a (Monteith, 1965). By inserting $\alpha = 1.26$ into equation (29) and assuming $r_s = 0$, which is an appropriate assumption in view of the saturated conditions of both the lake and swamp,

$$r_a = \frac{\gamma}{S} r_I / 0.26. \tag{31}$$

The variations of r_s and r_a with r_I and temperature is shown in Figure 9. Also shown is the average r_I computed for each surface from the average daily data. For all surfaces it is evident that the relationship between the resistances and α is temperature dependent. Furthermore, it is apparent from Figure 9 that the various resistances must have been relatively constant over each surface in order to conserve the consistency in α shown in Figures 7 and 8.

Since surface control over evaporation is relatively constant for each surface, simple models based on the concept of the equilibrium model can be utilized to estimate the actual evaporation for each as a function of temperature and available radiant energy.

As shown in Figure 8, evaporation from the ridge can be closely approximated by

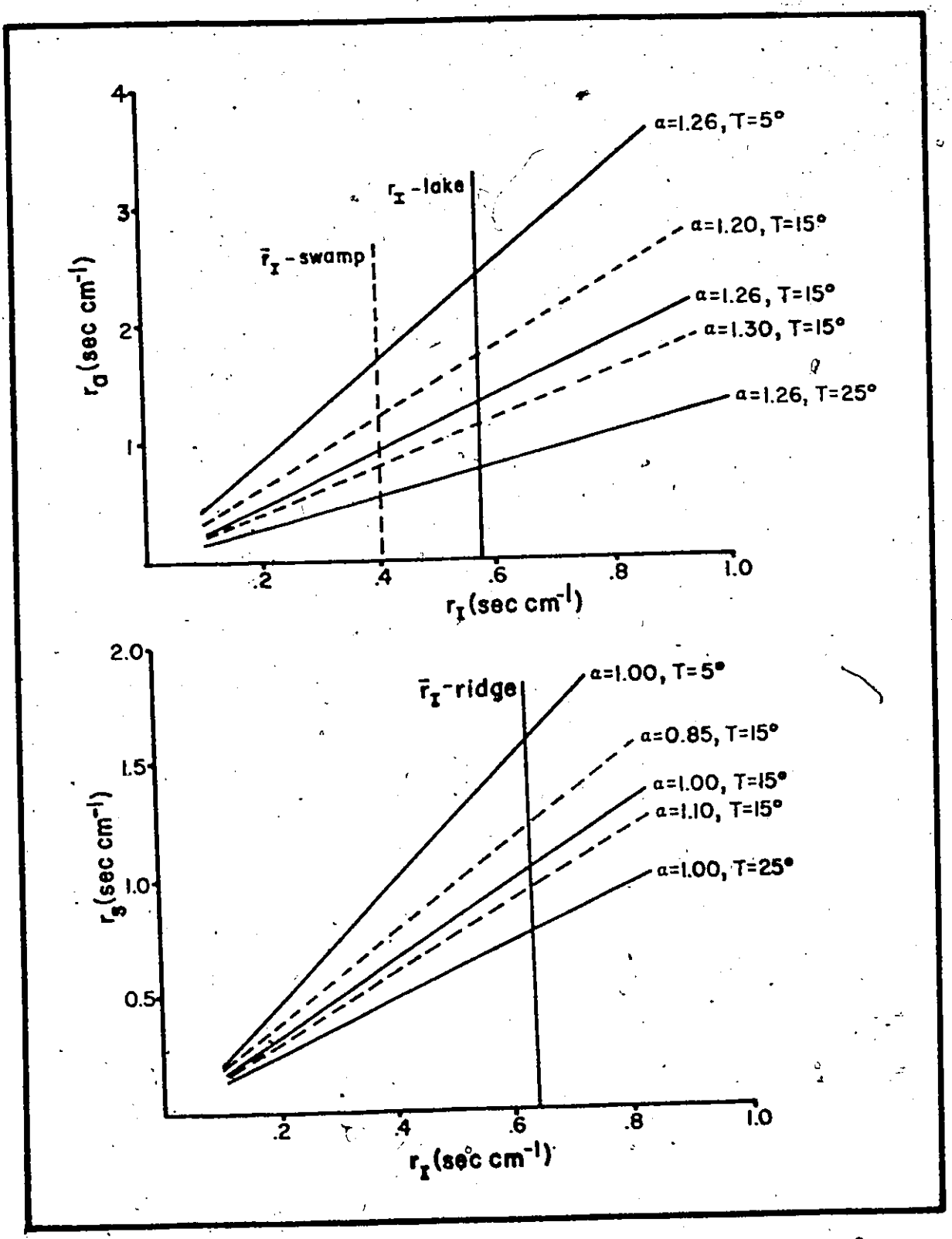

FIGURE 9a: Variation of r_a and r_I with Temperature and α when $r_s = 0$

FIGURE 9b: Variation of r_s and r_I with Temperature and α when LE is Independent of r_a

$$LE_{r'} = \frac{S}{S + \gamma} (Q^* - G), \tag{32}$$

while from the swamp and lake

$$LE_{s'} = LE_{l} = 1.26 \frac{S}{S + \gamma} (Q^* - G), \tag{33}$$

where the subscripts r', s' and l refer to the ridge, swamp and lake surfaces respectively. Hence from equations (32) and (33), estimation of the actual evaporation from a variety of surfaces in the Hudson Bay lowlands, requires only air temperature, which is closely related to $S/(S + \gamma)$, and Q^* and G. If these are known the evaporation estimates should be accurate to within 10 percent. The difficulty in applying these equations in this region stems from the lack of Q^* and G data which are not generally available. Few stations in northern Canada monitor Q^*, and those that do, measure the flux only over the drier upland areas. Similarly, there have been few measurements of G recorded for subarctic and tundra surfaces. In view of the dearth of data involving Q^* and G, application of evaporation models of the form expressed in equations (32) and (33) are limited to those areas where measurements are available. Hence, the need for a model that incorporates a few variables that are readily obtainable and which are relatively constant over a variety of surfaces is apparent.

CHAPTER V

DERIVATION AND TEST OF SOME SIMPLE EVAPORATION MODELS

1. Derivation of a New Model

The evaporative estimates could be simplified if Q* and G could be replaced with other meteorological parameters. Equation (20) can be modified by replacing Q* - G with a linear function of incoming solar radiation (K↓). A number of researchers have shown that $Q^* = a' + bK\downarrow$, where a' and b are obtained by regression analysis (Shaw, 1956: Monteith and Szeicz, 1961; Davies, 1967; Pritschen, 1967; Idso, Baker and Blad, 1969; Gay, 1971). To extend this linear form to include G requires an assumption about its magnitude and variability. For example, if G is small enough to be neglected or if G/Q* is relatively constant over time, Q* - G can be expressed in the linear form:

$$Q^* - G = a' + bK\downarrow. \tag{34}$$

Then, equilibrium evaporation can be rewritten as:

$$LE_{EQ} \quad \frac{S}{S + \gamma} (a' + bK\downarrow), \tag{35}$$

where a' is a regression constant and b is the regression coefficient. LE_{EQ} is now a function of temperature and incoming solar radiation; hence,

equation (20) becomes:

$$LE' = \frac{S}{S + \gamma} (A + BK\downarrow), \qquad (36)$$

where $A = \alpha a'$ and $B = \alpha b$.

Provided G and α can be considered constant the evaporation from a particular surface can be expressed as a function of temperature and incoming solar radiation. The advantages of LE' are twofold. First, it requires only a knowledge of the two variables of temperature and K↓, both of which are more readily available than either Q* or G. Second, both variables are fairly constant over a large variety of surface types within a radius of a few km, thus, facilitating the estimation of evaporation for several different surfaces in proximity to one measurement location.

2. Development of an Evaporation Model for the Ridge, Swamp and Lake Surfaces

As shown in Figure 2, G for the ridge and swamp is a small portion of Q*, and G/Q* is quite constant from day-to-day. For the lake, however, G often constitutes a large portion of Q* with the ratio G/Q* fluctuating considerably from day-to-day. In view of this, the form of equation (36) is unsuitable for computing LE for any lake on a daily basis. The possibility of estimating LE, using this approach, over periods greater than a day is explored further in a later section. For the ridge and swamp surfaces, however, the above results suggest that the evaporation can be approximated by a form of equation (36).

a. The Ridge and Swamp

Figures 10a and 10b show the linear relationships between half-hourly values of $Q^* - G$ and $K\downarrow$. By regression analysis

$$(Q^* - G)_R = -0.108 + 0.6364\ K\downarrow, \tag{37}$$

and

$$(Q^* - G)_S = -0.058 + 0.7365\ K\downarrow \tag{38}$$

for the ridge and swamp respectively. The agreement of each is supported by a high correlation coefficient and low standard error. Similar relationships for daily totals are shown in Figure 11.

Replacing $Q^* - G$ with the linear functions of $K\downarrow$ and using equations (32) and (33)

$$LE_R = \frac{S}{S + \gamma}\ (-0.108 + 0.7374\ K\downarrow) \tag{39}$$

for the ridge, and

$$LE_S = \frac{S}{S + \gamma}\ (-0.073 + 0.928\ K\downarrow) \tag{40}$$

for the swamp. Daily totals are obtained by summing the half-hourly values over the daylight period. All half-hourly and daily total relationships are in units of MJ m^{-2}.

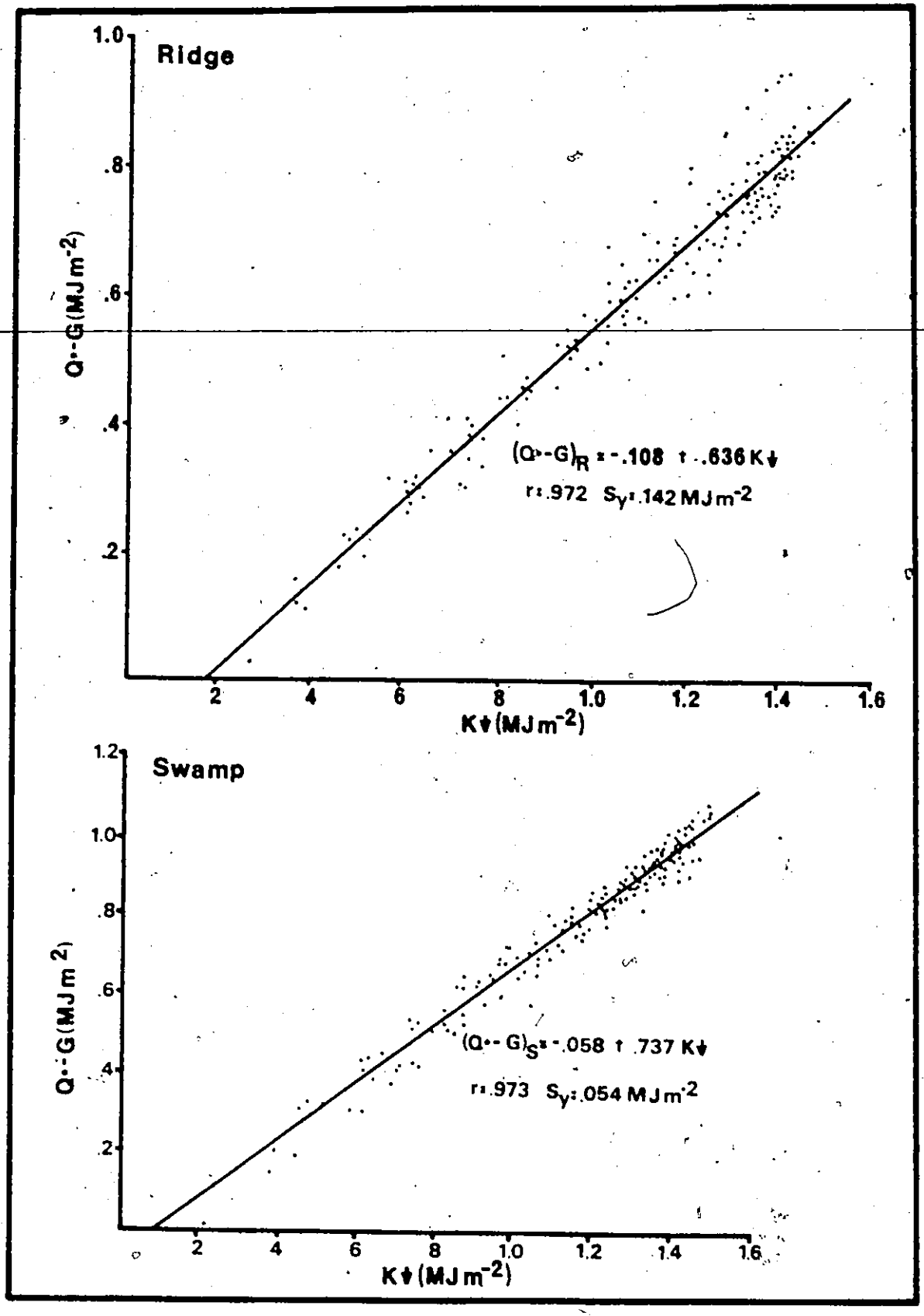

FIGURE 10: Comparison of Half-Hourly Q* - G with K↓ for the Ridge and Swamp Surfaces

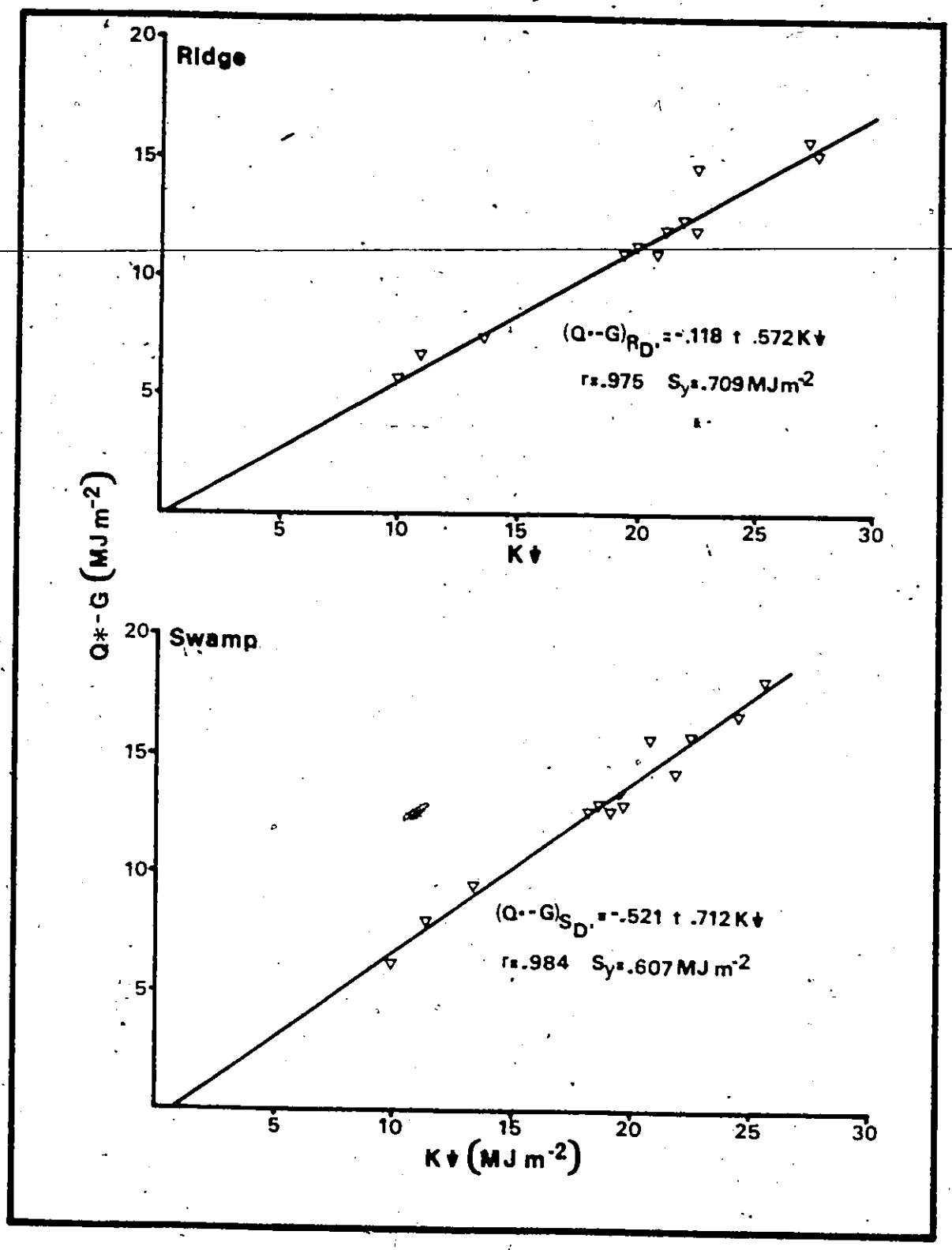

FIGURE 11: Comparison of Daily Totals of Q* - G with K↓ for the Ridge and Swamp Surfaces

The daily evaporation for the ridge and swamp can also be computed using the daylight total relationships shown in Figures 8 and 11. Hence, using the daylight total regression of $Q^* - G$ on $K\downarrow$, the daily evaporation can be expressed as:

$$LE_{R_{D'}} = \frac{S}{S + \gamma} (-0.1185 + 0.5715\ K\downarrow) \qquad (41)$$

for the ridge, and

$$LE_{S_{D'}} = \frac{S}{S + \gamma} (-0.6564 + 0.9059\ K\downarrow) \qquad (42)$$

for the swamp. Equations (39) and (40) are preferred to equations (41) and (42), since the larger sample size used in the establishment of the half-hourly relationships gives them a greater basis upon which to base the evaporation estimates.

b. Derivation of an Evaporation Model for the Lake

In attempting to develop an evaporation model for the shallow lake the problem of handling the large and variable heat storage term within the model framework must be solved. This can be done by eliminating the heat storage term (G_s) from the evaporation calculation by extending the time period over which the model is applied. For shallow tundra lakes $G_s \to 0$, over periods of a few days, due to rapid temperature fluctuations from day-to-day. If an appropriate time interval for which $G_s \to 0$ can be determined, a model similar to that expressed in equation (36) can be formulated.

An estimate of the fluctuation in the daily heat content of the lake, used in this study, in relation to the mean seasonal heat storage was obtained using the maximum and minimum temperature data shown in Figure 5, and the expression:

$$G_s = \rho C_w \bar{d} \, (T_{MW} - T_B). \tag{43}$$

C_w is the heat capacity of water, $\bar{d}$ is the average depth of the lake, T_{MW} is the mean daily lake temperature calculated as $(T_{max} + T_{min})/2$, and T_B is the mean temperature for the lake (12.8 C) obtained over the 55 days of measurement. Figure 12 shows that $G_s \rightarrow 0$ approximately 13 times between June 25 and August 14 for an average time interval of about 4.5 days. This suggests that an evaporation model, in the form of LE', should be applicable over periods as short as 4.5 days for a shallow lake. However, due to the large range of time intervals for which $G_s \rightarrow 0$, varying from 1-9 days, the use of periods of 1-2 weeks for the calculation of LE' would be more appropriate. A time interval of this length is necessary since G_s must be approximately zero in order to obtain accurate evaporation estimates. Hence, extending the calculation period forces the ratio G/Q^* to zero.

As shown in Figure 8c, the daily evaporation from the lake can be closely approximated by equation (33). Simplification was undertaken by expressing $Q^* - G$ as a linear function of $K\downarrow$, Remembering that G for the lake was determined as the sum of the heat storage term (G_s) and the flux of heat through the lake bottom (G_B), G_s was set to zero. Hence, by regression

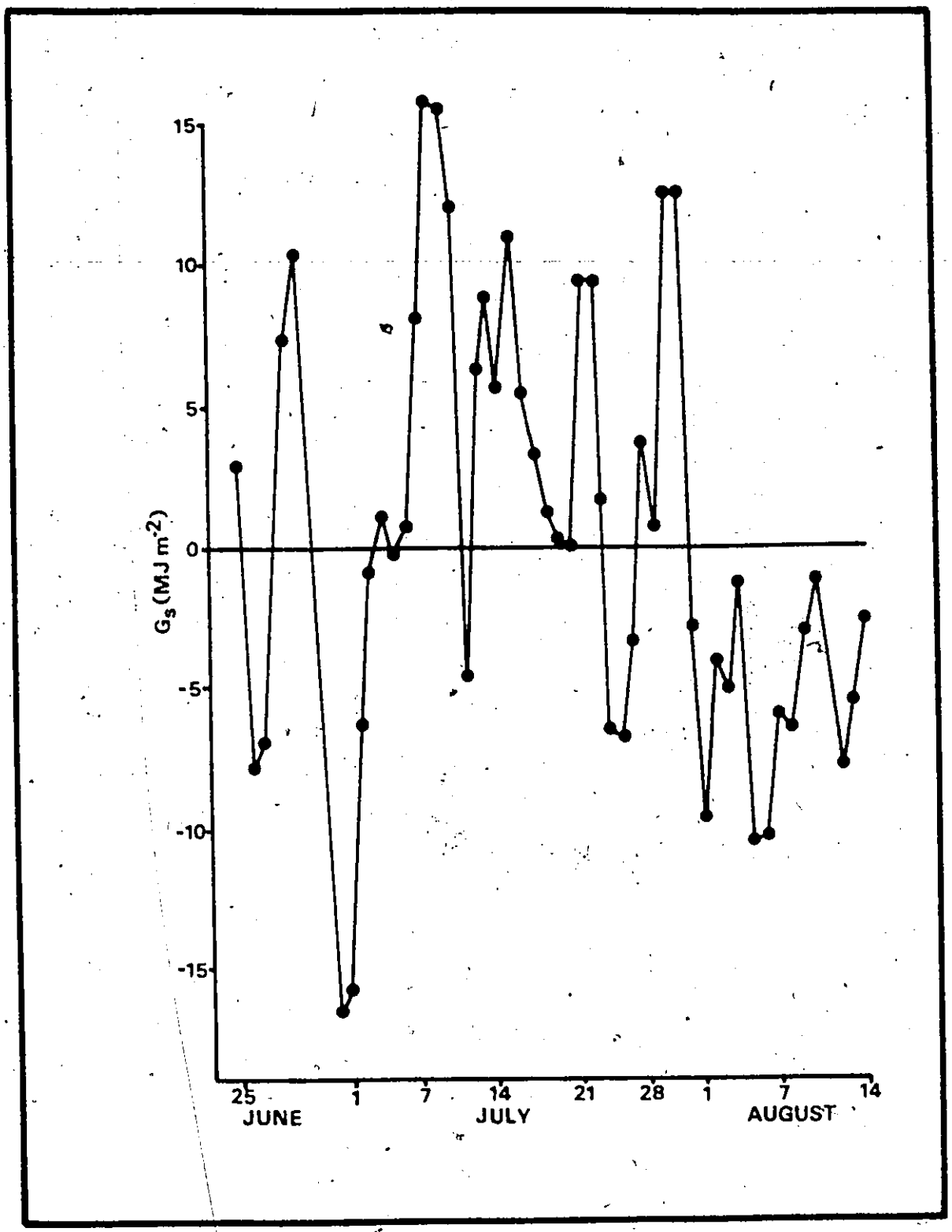

FIGURE 12: Seasonal Variation in the Daily Heat Storage Content of the Lake

$$(Q^* - G_B)_L = 0.9225 + 0.7353\ K\downarrow. \qquad (44)$$

Although the relationship, Figure 13a, is based on 12 days of data, comparison of equation (44) with the regression obtained using data collected by Weaver (1970), for the months of July, August and September over a shallow lake at Barrow, Alaska, shows similar results.

From equations (33) and (44)

$$LE_L = \frac{S}{S + \gamma}(1.624 + 0.9265\ K\downarrow), \qquad (45)$$

where LE_L, is the evaporation for the lake for a single day assuming $G_s = 0$. Summing LE_L over time intervals for which $G_s \to 0$, the evaporation from the lake can be computed as:

$$LE_{L'} = \sum_{i=7}^{n} LE_{L_i}, \qquad (46)$$

where $n > 7$ days, and LE_{L_i} is the evaporation for day i.

c. Model Requirements

Estimates of evaporation from equations (39), (40) and (45) requires a knowledge of the air temperature and incoming solar radiation. $K\downarrow$ represents the sum total of incoming solar radiation for the period of calculation. The temperature required in LE' should be the mean of the wet and dry bulb temperatures, since these are the temperatures used in the evaluation of S. Wilson and Rouse (1972) have shown that provided

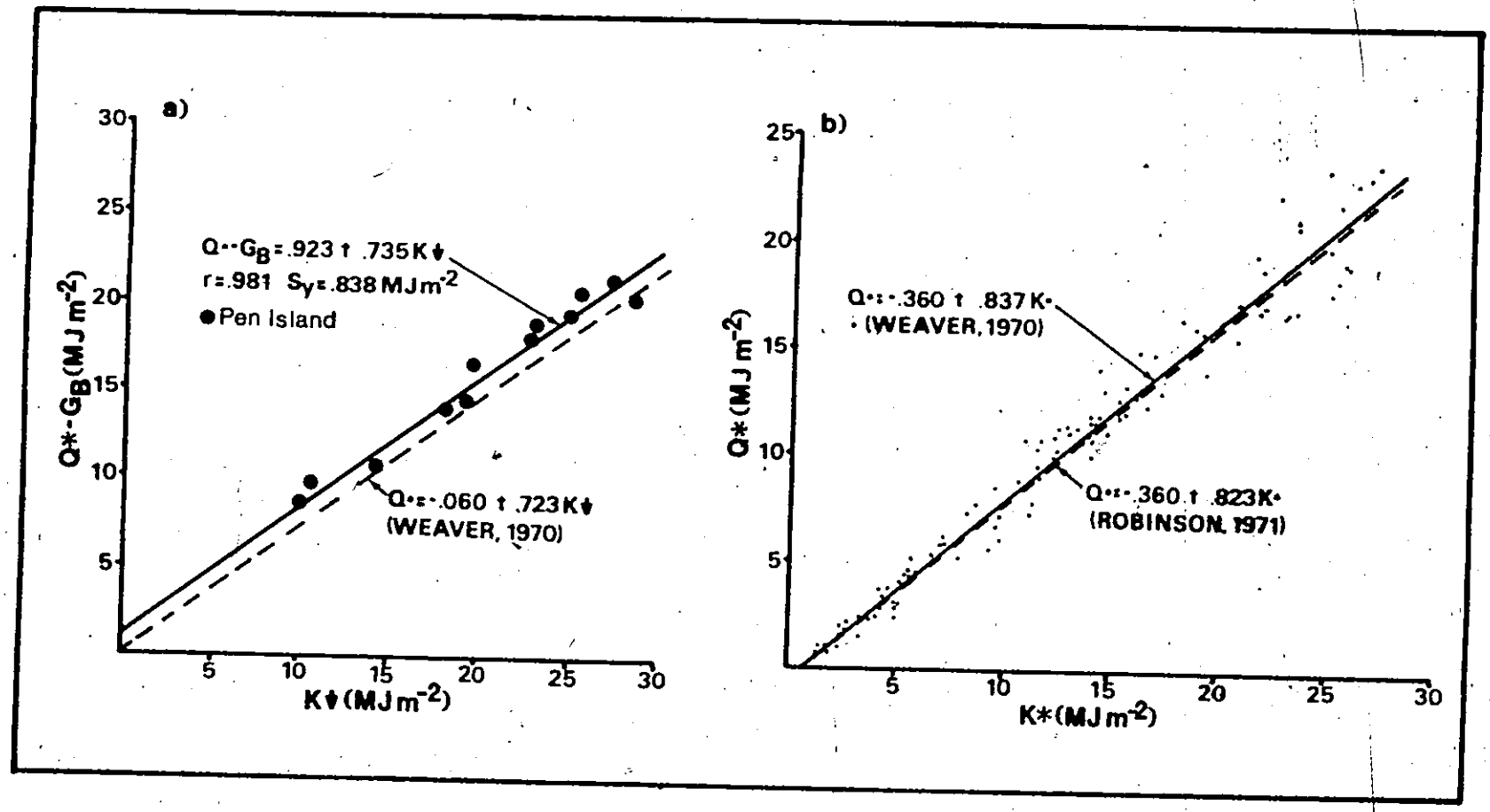

FIGURE 13a: Comparison of Daily Totals of Q* - G with K↓ for the Lake

FIGURE 13b: Comparison of Q* with K* for a Shallow Lake at Barrow, Alaska

the wet bulb depressions are not too great, the ratio $S/(S + \gamma)$ can be closely approximated by a linear expression of the screen height air temperature. Rouse and Stewart (1972), in a similar fashion, found that over the temperature range 6.6 - 27.7 C

$$\frac{S}{S + \gamma} = 0.434 + 0.012\ T_A, \tag{47}$$

where T_A is the screen height air temperature. Over this temperature range a change of 1 C alters the ratio by only 0.012. Therefore, although the proportionality factor is temperature-dependent and air temperature changes with height, the actual height of the temperature measurement is not critical (Wilson and Rouse, 1972). As a result, the average screen-height air temperature over the period of calculation is sufficient for the calculation of S in evaluating LE'. Thus, with a simple knowledge of T_A and K↓ it may be possible to estimate daily evaporation for subarctic and tundra surfaces, which exhibit similar characteristics to those of the ridge and swamp, to within 10 percent. A similar accuracy should also be possible for the shallow lake. However, to attain this reliability the period of calculation should be extended to weekly or two-weekly time intervals due to the variability of the heat storage term.

3. Test of the Evaporation Models

To test the validity of equations (39) and (40) as general models for estimating evaporation for various subarctic and tundra surfaces, values of measured LE were obtained from other sites of similar latitude.

A test of LE_L in a similar altitude was not possible due to lack of data. Instead, the model was tested in a more southerly location employing extensive data acquired by the Atmospheric Environment Service in an evaporation investigation at Perch Lake, a shallow lake in Ontario (lat. 46°03'N, long. 77°23'W).

a. Test of the Ridge Model

Data to test LE_R were obtained from Rouse and Kershaw (1971) and Rouse and Stewart (1972). The same ridge, used in this experiment only at a different location, was utilized by Rouse and Stewart for their energy budget calculations during July and August, 1971. Rouse and Kershaw obtained LE estimated at Hawley Lake, a site approximately 300 km ESE of Pen Island (lat. 54°20'N, long. 84°20'W).

The two surfaces investigated by Rouse and Kershaw differed significantly from that at Pen Island. One consisted of a dense natural lichen surface composed almost entirely of *Cladina alpestris*, averaging .11 m in thickness. The other was an 18 year old lichen burn that was just beginning to be revegetated.

Figure 14 shows the relationship between calculated daily values, LE_R, and actual LE measured for all surfaces at Hawley Lake and Pen Island. The model performs well as shown by the correlation coefficient of 0.971 and standard error of $\pm$ 0.483 MJ m^{-2} day^{-1} for the 27 days of comparison.

These results support the use of the generalized evaporation model expressed in equation (39) in estimating the daily evaporation from lichen-covered and burned subarctic surfaces.

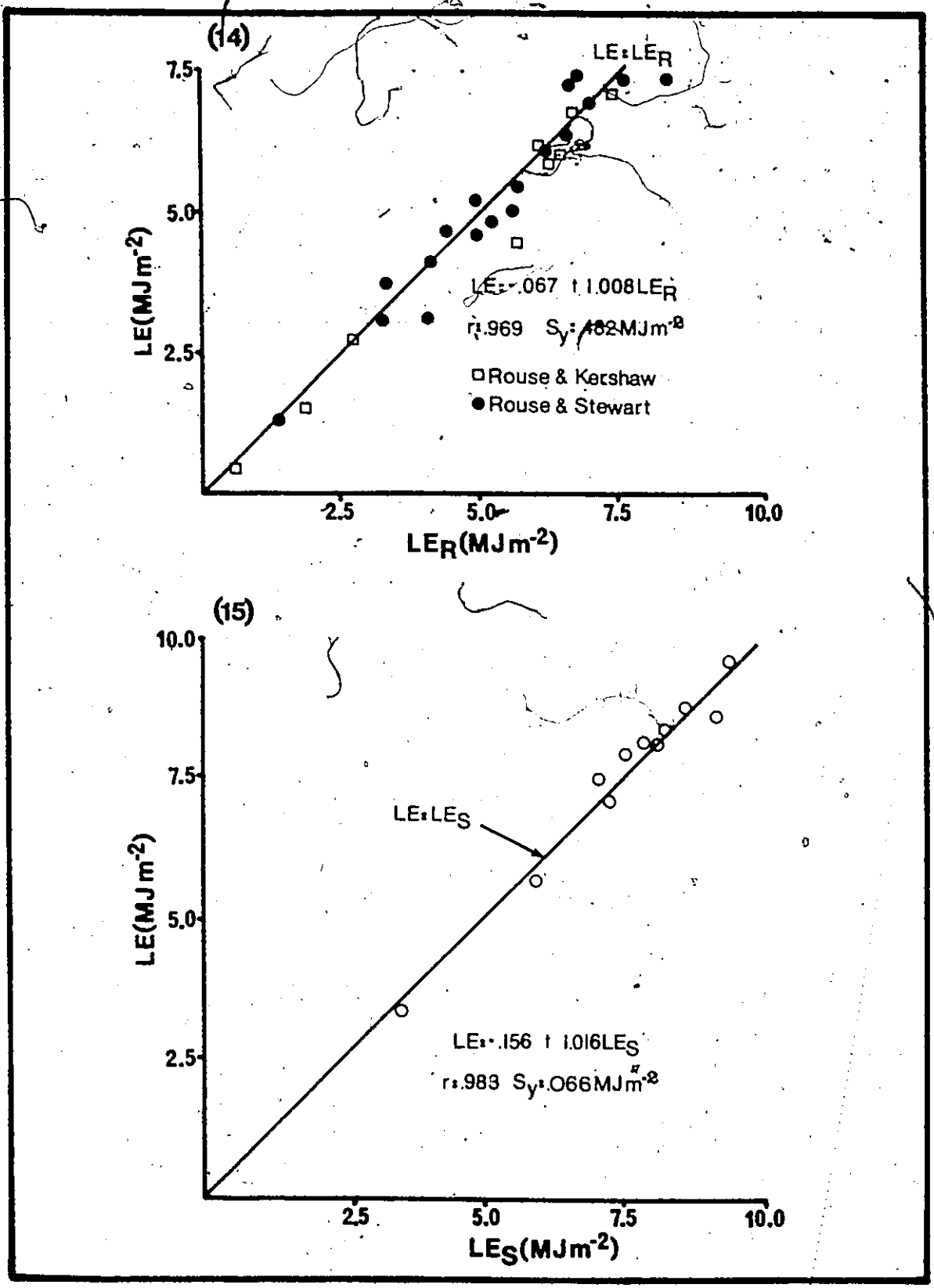

FIGURE 14: Comparison of Daily LE to LE_R at Hawley Lake and Pen Island

FIGURE 15: Comparison of Daily LE to LE_S at Thor Lake, N.W.T.

b. Test of the Swamp Model

Data to test LE_s were obtained during July, 1974 over a swamp surface in the vicinity of Thor Lake, N.W.T. (lat 60°N, long. 107°W) approximately 135 km NE of Uranium City, Saskatchewan. The swamp surface was similar in all respects to that at Pen Island with the surface vegetation dominated by sedges and grasses. The main difference between the two surfaces was in the depth of water which was 100-150 mm at Thor Lake as compared to 10-30 mm at Pen Island. The greater depth of water at Thor Lake presented no problems in using the daily energy budget data to test LE_s as analysis of the heat storage component revealed that it was small in comparison to the magnitude of Q^*.

The results of the comparison of LE_s with measured daily values of LE are shown in Figure 15. The excellent agreement shows that the swamp model performs well, supporting the generalized evaporation model, expressed in equation (40) for estimating the daily LE from saturated vegetated surfaces where the heat storage component is negligible.

c. Test of the Lake Evaporation Model

To the writer's knowledge, no lake evaporation data are available to test the applicability of LE_L in high latitudes. However, several years of data were available from a shallow lake at Perch Lake, Ontario (Ferguson and Den Hertog, 1975), located approximately 2 km SW of the Chalk River Atomic Energy of Canada Laboratories.

Perch Lake is similar in size and depth to the lake at Pen Island, being almost circular with a surface area of $4.5 \times 10^5 m^2$ and a mean

depth of 2 m. A dense forest averaging 15 to 20 m in height encircled the lake at a distance from shore of 30 to 40 m.

Evaporation, heat storage and radiation data were available for June through September for 1970, 1971 and 1972. The data record was not complete, however, as several weeks of measurements were often missing due to instrumental failure. Available measurements included daily totals of ΔG_s, Q*, LE by the energy budget method, and average daily water surface temperature and air temperature. Daily totals of K↓, required for use in LE_L, were not measured. This created a problem since the nearest station measuring K↓ was located 200 km distance at Ottawa. Differences between daily values of Q* for a grass surface at Chalk River and one at Ottawa were as large as 60%. On average the former were smaller by 10% (G. Den Hertog - personal communication). In lieu of K↓ measurements, an empirical expression derived by Robinson, *et al.* (1972) was used in the derivation of K↓, where:

$$Q^* = 0.368 + 0.823\ K^*, \qquad (48)$$

$$r = 0.986 \qquad S_y = 0.977\ MJ\ m^{-2}\ day^{-1}$$

and K* is the net shortwave radiation. As seen in Figure 13b, Robinson's expression relating Q* to K* for Lake Ontario, compares quite favourably with that obtained from data collected by Weaver (1970), for a shallow lake at Barrow, Alaska.

Since $K^* = (1 - a)\ K\downarrow$, where a is the lake surface albedo, equation (48) can be solved for K↓ as:

$$K\downarrow = \frac{0.447 + 1.215\ Q^*}{(1 - a)} \quad . \qquad (49)$$

Albedo values over Lake Ontario remain fairly constant at approximately 0.08 from June through September (Nunez, *et al.*, 1971; Davies and Schertzer, 1974). Similar values have been recorded at Lake Mead (Harbeck, *et al.*, 1959) and Lake Hefner (Anderson, 1954) in the southwestern United States, as well as, in Alaska (Weaver, 1970). Substituting a = 0.08 into equation (49), the daily estimates of K↓ for Perch Lake were computed from

$$K\downarrow = 0.486 + 1.321\ Q^* . \qquad (50)$$

Figure 16a shows the relationship between two-weekly totals of LE_L and measured values of LE for Perch Lake. It is apparent that the model performs satisfactorily. Furthermore, when the calculation period is lengthened to a month, Figure 16b, the model performance is improved. These results indicate the generalized evaporation model expressed in equation (45) is reliable in estimating the two-weekly and monthly totals of evaporation from shallow lakes.

4. Significance of the Results

The good agreement between measured LE and LE_R for the lichen covered and burned surfaces, LE_s for the swamp, and LE_L for the shallow lake, is important. Previous discussion has shown that air temperature and available radiant energy are the prime controls over evaporation from

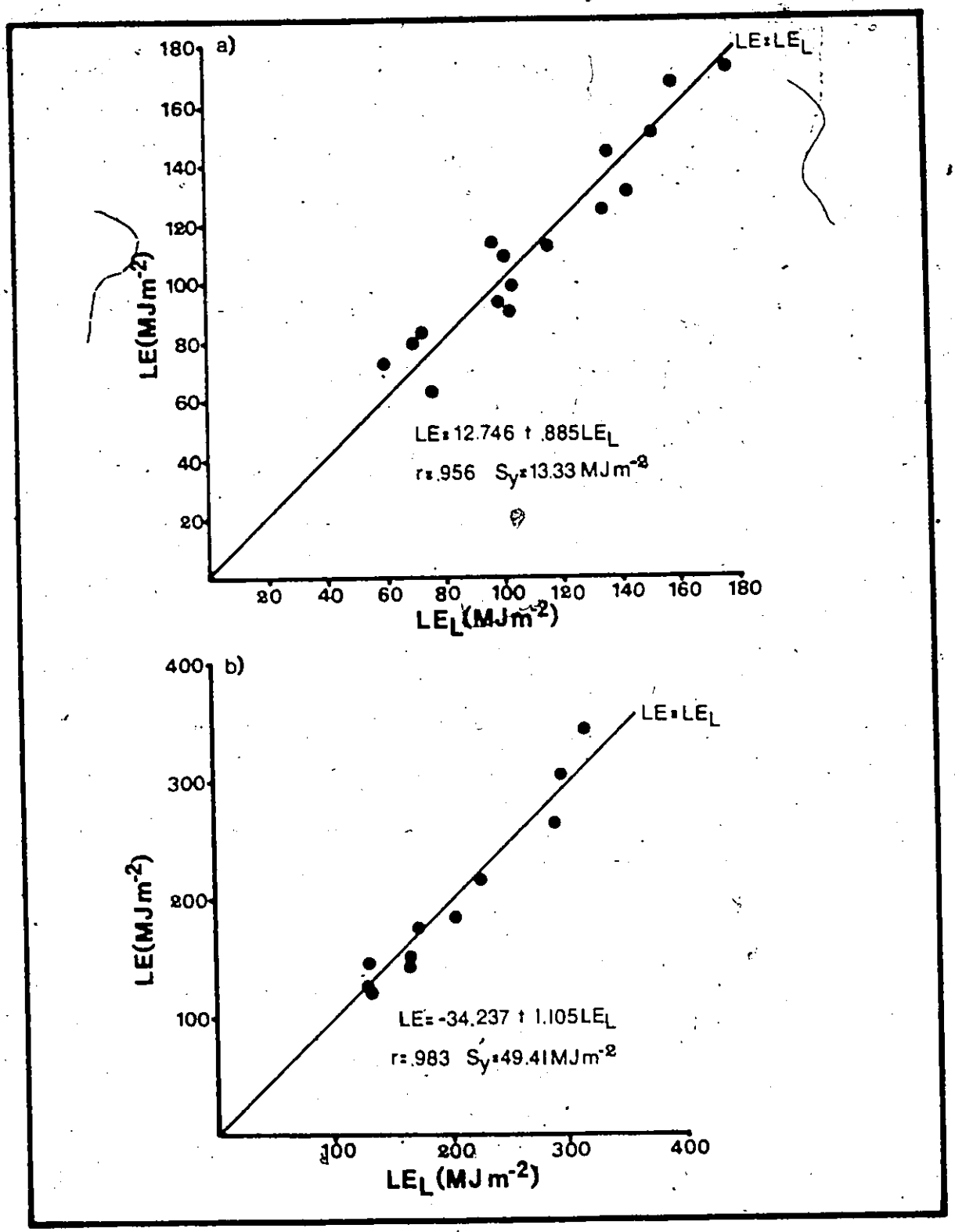

FIGURE 16: Comparison of Two-Weekly and Monthly Totals of LE to LE$_L$ at Perch Lake, Ontario.

the different surfaces investigated in this study. It is apparent from the successful testing of the three models, LE_R, LE_s and LE_L that evaporation for the three surfaces can be estimated accurately as a function of temperature and incoming solar radiation.

Values of α are similar for the various swamp and lake surfaces. Figure 17 shows the comparison of daily LE with equilibrium evaporation estimates for the swamp at Pen Island and Thor Lake, and the shallow lakes at Pen Island and Chalk River. For Perch Lake the two-weekly totals of LE and LE_{EQ} were divided by 14 to produce daily estimates for comparison with the other surfaces. The results of this study add further verification to the value of $\alpha = 1.26$ for conditions of potential evaporation. The results of Figure 17 suggest that α may equal 1.26 for a variety of saturated surfaces in high latitudes.

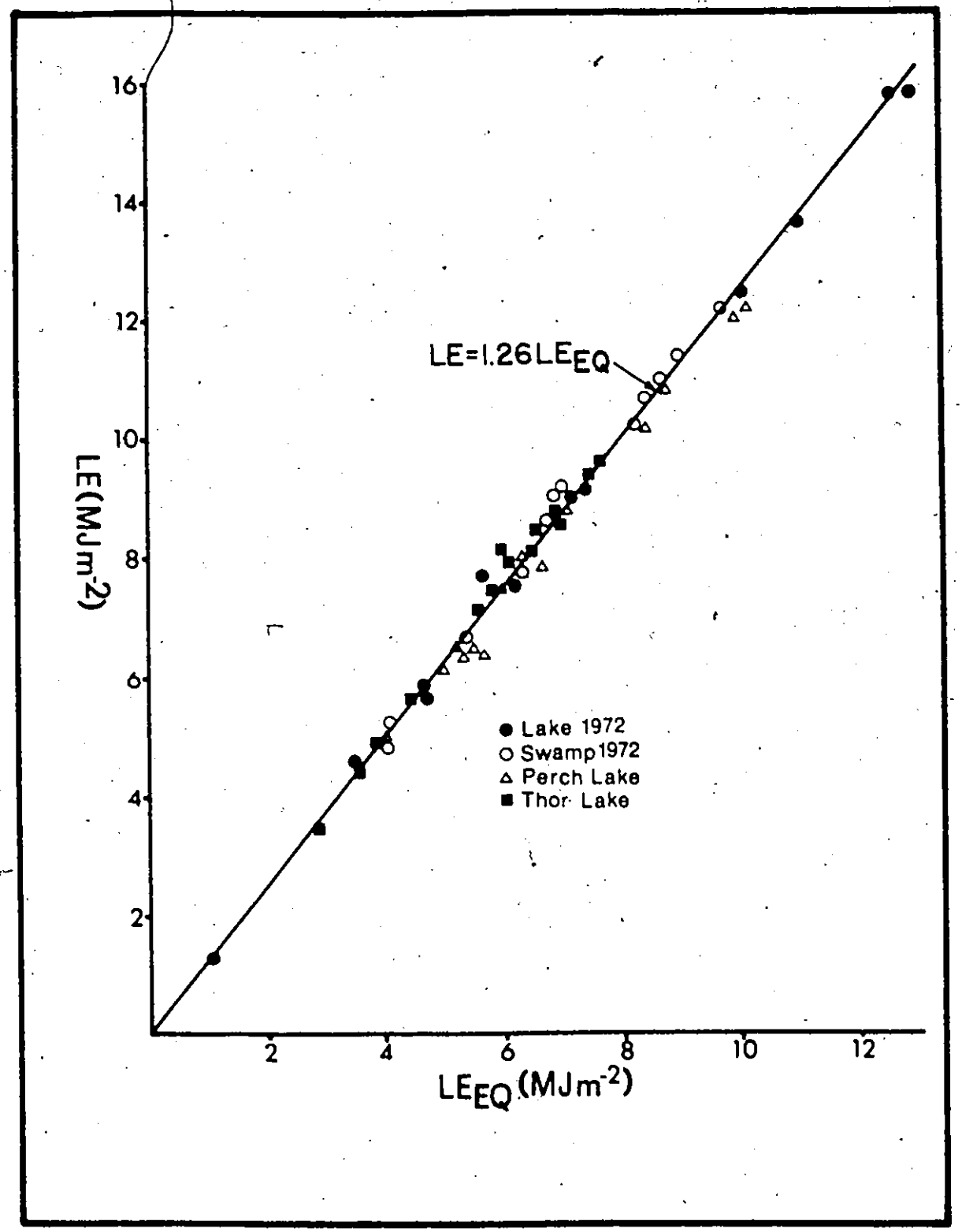

FIGURE 17: Comparison of Daily Totals of LE with LE_{EQ} for the Various Lake and Swamp Surfaces

CHAPTER VI

SUMMARY AND CONCLUSIONS

The energy balance method was used to estimate the half-hourly and daily totals of evaporation for three different surfaces. The three surfaces, located adjacent to East Pen Island in Northern Ontario, comprised a lichen-dominated raised beach ridge, a swamp and a shallow lake. Computations showed that for the ridge surface 54% of the daily net radiation was utilized in the evaporative process. Evaporation from the swamp comprised 66% of Q* while 55% was used over the lake. For the lake approximately 25% of the daily Q* was used in warming the lake water. Much of this is later released in the form of LE. The sensible heat component comprised a significant proportion of Q* over each surface, averaging 38, 25 and 18 percent for the ridge, swamp and lake surfaces. Corresponding Bowen ratios averaged 0.698, 0.380 and 0.365 respectively.

Half-hourly and daily evaporation estimates from the equilibrium model were compared to corresponding energy balance values in order to test the hypothesis that the surface control over evaporation was constant in time and that temperature and radiant energy were the main variable controls affecting the day-to-day changes in LE. The equilibrium model was found to consistently overestimate the actual evaporation for the ridge by 1-4%, further substantiating the use of LE_{EQ} in

estimating the evaporation for moderately dry surfaces. Conversely, the half-hourly and daily totals consistently underestimated LE by 20 and 24% for the swamp, and 21 and 19% for the lake. For both the lake and swamp an α multiplier of 1.26 brought equilibrium evaporation into close agreement with the actual evaporation. This value agrees with the value of α found to apply to a variety of wet surfaces in mid-latitude areas.

A set of models has been developed, whereby, the two commonly measured variables of temperature and incoming solar radiation have been substituted into the equilibrium format. Tests of the models for natural lichen and burned surfaces at Hawley Lake and Pen Island, LE_R, and a swamp at Thor Lake, N.W.T., LE_S, gave excellent agreement when compared to actual evaporation. Both computed the daily totals to within 6 percent. The test of the lake model, LE_L, for the shallow waters of Perch Lake gave a good comparison to measured evaporation, estimating the two-weekly and monthly totals within 9 and 5% respectively.

In conclusion, the results of this study show that the daily evaporation can be estimated as a function of equilibrium evaporation within 5% for the ridge, swamp and lake surfaces. For the ridge, where a strong resistance to evaporation was found, in conjunction with the similar findings of Rouse and Stewart (1972) for diverse lichen and burned surfaces, the results of this study substantiate the use of the equilibrium model for determining the evaporation from upland dry surfaces in the subarctic and tundra region. For saturated surface conditions, exhibited by the swamp and lake at Pen Island, the ratio of actual to equilibrium

evaporation is equivalent to 1.26. In conjunction with the near identical ratios obtained at Thor Lake and Chalk River, this study shows that the Priestley and Taylor (1972) value of $\alpha = 1.26$ applies to wet surfaces, containing free standing water, in high-latitude areas. For these surface types the Priestley and Taylor model can be used to estimate the daily evaporation within 5 percent.

The results of this study further show that the evaporation for a ridge, swamp and shallow lake can be accurately estimated as a function of temperature and incoming solar radiation. Tests of models based on this concept show the following. For upland surfaces exhibiting a strong resistance to evaporation, in the presence of abundant surface soil moisture, the daily evaporation can be estimated within 6%. For swamp surfaces, consisting of sedge and grass vegetation, and maintaining from 10-150 mm of free standing water, the evaporation can be determined to within 5% on a daily basis. For shallow lakes, with depths between 0.5 and 2 m, and providing the heat storage term approaches zero, the evaporation can be estimated within 10% for periods of two weeks to a month.

APPENDIX A

LIST OF SYMBOLS

1. Roman Capital Letters

A Regression constant ($J\ m^{-2}$)

B Regression coefficient (dimensionless)

C Heat capacity ($J\ g^{-1}\ C^{-1}$)

C_p Specific heat of air at constant pressure ($J\ m^{-2}\ C^{-1}$)

C_R Heat capacity of the ridge soil ($J\ g^{-1}\ C^{-1}$)

C_S Heat capacity of the swamp soil ($J\ g^{-1}\ C^{-1}$)

C_W Heat capacity of water ($J\ g^{-1}\ C^{-1}$)

D Wet bulb depression (C)

D' Subscript referring to daily totals

E Quantity of evaporated water (mm)

G Heat flux across the earth-atmosphere interface ($J\ m^{-2}$)

G_B Heat flux into the lake bottom ($J\ m^{-2}$)

G_L Heat flux into the lake ($J\ m^{-2}$)

G_s Heat storage content of the lake ($J\ m^{-2}$)

H Sensible heat flux ($J\ m^{-2}$)

K Incoming solar radiation ($J\ m^{-2}$)

K* Net solar radiation ($J\ m^{-2}$)

K_H Eddy diffusivity of heat ($m^2\ sec^{-1}$)

K_W Eddy diffusivity of water ($m^2\ sec^{-1}$)

L Latent heat of vapourization (J mm)

LE Evaporation ($J\ m^{-2}$)

LE_{EQ} Equilibrium evaporation ($J\ m^{-2}$)

LE_L Evaporation model for the lake ($J\ m^{-2}$)

LE_R Evaporation model for the ridge ($J\ m^{-2}$)

LE_S Evaporation model for the swamp ($J\ m^{-2}$)

LE' Evaporation model ($J\ m^{-2}$)

PLE Potential evaporation ($J\ m^{-2}$)

Q^* Net radiation ($J\ m^{-2}$)

S Slope of the saturation vapour pressure-temperature curve

S_y Standard error of the estimate ($J\ m^{-2}$)

T Dry bulb temperature (C)

T_A Screen height air temperature (C)

T_B Mean seasonal water temperature for the lake (C)

T_L Temperature of the lake (C)

T_M Mean temperature (C)

T_s Surface temperature (C)

T_w Wet-bulb temperature (C)

T_{WT} Weighted average temperature (C)

V Output (mV)

X_m Volumetric fraction of mineral matter (dimensionless)

X_o Volumetric fraction of organic matter (dimensionless)

2. Roman Lower Case Letters:

a Albedo (dimensionless)

a' Regression constant ($J\ m^{-2}$)

b Regression coefficient (dimensionless)

$\bar{d}$ Average depth of the lake (m)

e Vapour pressure (pa)

δe Saturation vapour pressure deficit (pa)

e_s Saturation vapour pressure (pa)

h Windspeed transfer coefficient

i Subscript referring to time

l Subscript referring to the lake

r Correlation coefficient (dimensionless)

r_a Aerodynamic resistance (m^{-2} sec^{-1})

r_I Climatological resistance (m^{-2} sec^{-1})

r_s Surface resistance (m^{-2} sec^{-1})

r' Subscript referring to the ridge

s' Subscript referring to the swamp

t Time (hr)

z Height (m)

3. Greek Letters and Other Symbols:

β Bowen ratio (dimensionless)

γ Psychrometric constant (pa C^{-1})

α Ratio of actual evaporation to equilibrium (dimensionless)

ρ density (g m^{-3})

θ Volumetric fraction of water (dimensionless)

Δ Gradient (various units)

APPENDIX B

APPENDIX B

RADIOMETER CALIBRATIONS

LOCATION	FLUX	INSTRUMENT NO.	CALIBRATION ($J.mV^{-1}$) LONGWAVE	SHORTWAVE
Lake	Q*	6633	164.85	147.28
Swamp	Q*	6635	155.64	137.65
Ridge	Q*	6636	157.32	143.51

APPENDIX C

ERROR ANALYSIS OF THE TEMPERATURE AND HUMIDITY AND RESULTANT ERRORS IN LE

1. Temperature

The dry and wet-bulb temperature data were reduced by:

$$T = C_c V, \tag{C-1}$$

where C_c is the calibration constant and V is the electrical output of the recording instrument. The main errors involved in the temperature measurements are incorporated in the calibration constant and the recorder output. Other sources of error, such as, those due to radiational heating of the temperature sensors, inadequate sampling and the human error involved in the data extraction from chart recordings, for the purposes of this study could not be assessed.

The maximum absolute error in T, δT, can be evaluated by partially differentiating equation (C-1) with respect to C_c and V, such that:

$$\delta T = \frac{\partial T}{\partial C_c} \delta C_c + \frac{\partial T}{\partial V} \delta V, \tag{C-2}$$

where δC_c and δV are the absolute errors in the calibration constant and recorder output, and $\partial T/\partial C_c$ and $\partial T/\partial V$ are the partial derivatives of temperature with respect to the calibration constant and recorder output respectively. Following the procedure of Cook and Rabinowicz (1963),

dividing equation (C-2) by T and taking the root mean square solution, the relative error in T was evaluated as:

$$\left(\frac{\delta T}{T}\right) \text{ R.M.S.} = \pm\left[\left(\frac{\delta C_c}{C_c}\right)^2 + \left(\frac{\delta V}{V}\right)^2\right]^{1/2} \quad \text{(C-3)}$$

Temperature gradients between various levels of measurement were calculated as

$$T = T_z - T_{z-1}, \quad \text{(C-4)}$$

where ΔT is the difference in temperature between the heights z and z-1. Differentiating equation (C-4) with respect to T_z and T_{z-1}, the absolute error in ΔT, $\delta\Delta T$, is

$$\delta\Delta T = \frac{\partial \Delta T}{\partial T_z}\,\delta T_z + \frac{\partial \Delta T}{\partial T_{z-1}}\,\delta T_{z-1}, \quad \text{(C-5)}$$

Dividing by ΔT, and computing the root mean square solution, the relative error is given by

$$\left(\frac{\delta \Delta T}{\Delta T}\right) \text{ R.M.S.} = \pm\left[\left(\frac{\delta T_z}{\Delta T}\right)^2 + \left(\frac{\delta T_{z-1}}{\Delta T}\right)^2\right]^{1/2}. \quad \text{(C-6)}$$

For the calculation of equation (C-3) and (C-6), absolute errors of 0.017 C and 0.01 mV were assigned to δC_c and δV respecitvely. The former value represents the standard error of the estimate obtained from the regression of T on V, while the latter, represents the recorder accuracy

for the 10mV full scale range. Absolute and relative errors in T were calculated over the temperature range 0-30 C. These were then utilized in computing the absolute and relative errors in ΔT for temperature gradients ranging from 0.1 to 2.0 C, and absolute temperatures in the vicinity of 5, 15 and 25 C respectively. The results are shown on Table A.

2. Humidity

The vapour pressure gradient was calculated using equation (8). Ignoring the small errors in S caused by the errors in T and T_w, and differentiating with respect to T and T_w, the absolute error in the vapour pressure gradient is obtained from

$$\delta \Delta e = \frac{\partial \Delta e}{\partial \Delta T} \delta \Delta T + \frac{\partial \Delta e}{\partial \Delta T_w} \delta \Delta T_w . \qquad (C-7)$$

Utilizing the root mean square solution to equation (C-7), the relative error in Δe was computed from

$$\left(\frac{\delta e}{\Delta e}\right) \text{R.M.S.} = \pm \left[\left(\frac{(S + \gamma)\ \delta \Delta T_w}{\Delta e} \right)^2 + \left(\frac{\gamma \delta \Delta T}{\Delta e} \right)^2 \right]^{1/2} . \qquad (C-8)$$

Using an absolute dry bulb temperature of 15 C, which was the average air temperature over all surfaces during the experiment, the absolute and relative errors in Δe were computed over the wet-bulb depression range 1.0 to 10.0 C. For these calculations the absolute error varied from 8 to 12 pa.

TABLE A

ABSOLUTE AND RELATIVE ERRORS IN T AND ΔT

T (°C)	ABSOLUTE ERROR (°C)	RELATIVE ERROR (%)
5.0	.0291	.581
10.0	.0357	.357
15.0	.0450	.300
20.0	.0558	.279
25.0	.0675	.270
30.0	.0792	.264

ABSOLUTE ERROR IN ΔT (°C)

ΔT (°C) \ T (°C)	5	15	25
0.10	.0411	.0637	.0955
0.50	.0409	.0629	.0953
1.00	.0408	.0623	.0939
2.00	.0405	.0609	.0922

RELATIVE ERROR IN ΔT (%)

ΔT (°C) \ T (°C)	5	15	25
0.10	41.08	63.70	95.46
0.50	8.18	12.56	19.09
1.00	4.08	6.23	9.39
2.00	2.03	3.04	4.61

3. Errors in Q* and G

In this experiment an error of 5% was assigned to Q* (Fuchs and Tanner, 1970). An error of 10% was assigned to G for the ridge and swamp (Fuchs and Tanner used a similar value), while for the lake, the relative error in G was computed to be approximately 10%. This was attained by differentiating equation (25a) with respect to: the average lake depth ($\bar{d}$), the average lake temperature change (ΔT_L) and the heat flux through the lake bottom, such that, the absolute error in G_L, δG_L, was:

$$\delta G_L = \frac{\partial G_L}{\partial G_B} \delta G_B + \frac{\partial G_L}{\partial \Delta T_L} \delta \Delta T_L + \frac{\partial G_L}{\partial \bar{d}} \delta \bar{d}. \qquad \text{(C-9)}$$

The relative error was then obtained by dividing equation (C-9) by G_L, and taking the root mean square solution, such that

$$\left(\frac{\delta G_L}{G_L}\right)_{R.M.S.} = \pm \left[\left(\frac{\partial G_L}{\partial G_B}\right)^2 \left(\frac{\delta G_B}{G_L}\right)^2 + \left(\frac{\partial G_L}{\partial \Delta T_L}\right)^2 \left(\frac{\delta \Delta T_L}{G_L}\right)^2 + \left(\frac{\partial G_L}{\partial \bar{d}}\right)^2 \left(\frac{\delta \bar{d}}{G_L}\right)^2 \right]^{1/2}. \qquad \text{(C-10)}$$

For this experiment, since G_B was estimated from the rate of frost retreat under the lake, it was assumed that G_B was accurate only to within 25%. In addition, it was assumed that ΔT_L was within 0.1 C and that the average lake depth was known to within 0.05 m.

4. Errors in LE

The evaporation for each surface was evaluated using equation (6). Partially differentiating LE with respect to Q*, G, ΔT, and Δe, the absolute errors in the evaporation estimates were determined from

$$\delta LE = \frac{\partial LE}{\partial Q^*}\,\delta Q^* + \frac{\partial LE}{\partial G}\,\delta G + \frac{\partial LE}{\partial \Delta T}\,\delta \Delta T + \frac{\partial LE}{\partial \Delta e}\,\delta \Delta e, \qquad \text{(C-11)}$$

and the relative errors from

$$\frac{\delta LE}{LE}\ \text{R.M.S.} = \pm \left[\left(\frac{\partial LE}{\partial Q^*}\right)^2 \left(\frac{\delta Q^*}{LE}\right)^2 + \left(\frac{\partial LE}{\partial G}\right)^2 \left(\frac{\delta G}{LE}\right)^2 + \left(\frac{\partial LE}{\partial \Delta T}\right)^2 \left(\frac{\delta \Delta T}{LE}\right)^2 + \left(\frac{\partial LE}{\partial \Delta e}\right)^2 \left(\frac{\delta \Delta e}{LE}\right)^2 \right]^{1/2} . \qquad \text{(C-12)}$$

where:

$$\frac{\partial LE}{\partial Q^*} = (1 + \gamma \Delta T/\Delta e)^{-1}, \qquad \text{(C-13)}$$

$$\frac{\partial LE}{\partial G} = (1 + \gamma \Delta T/\Delta e)^{-1}, \qquad \text{(C-14)}$$

$$\frac{\partial LE}{\partial \Delta T} = \frac{Q^* - G}{(1 + \gamma \Delta T/\Delta e)^2} \cdot \gamma/\Delta e, \qquad \text{(C-15)}$$

and

$$\frac{\partial LE}{\partial \Delta e} = \frac{-\ Q^* - G}{(1 + \gamma \Delta T/\Delta e)^2} \cdot \gamma \Delta T/\Delta e^2 . \qquad \text{(C-16)}$$

Evaluation of equation (C-11) showed that in the presence of large temperature gradients, an accuracy of 7-12% was attained in the LE estimates for all surfaces.

APPENDIX D

DAILY ENERGY BALANCE AND EQUILIBRIUM

EVAPORATION DATA FOR PEN ISLAND

The following symbols are used:

ID	= Date (day-month)
Q^*	= Net radiation
G	= Soil heat flux
LE	= Evaporation
LE_{EQ}	= Equilibrium evaporation
α	= Ratio of actual to equilibrium evaporation (dimensionless)
β	= Bowen ratio (dimensionless)
T_A	= Average screen height air temperature (C)

All fluxes are in MJ m^{-2} day^{-1} and are considered positive if directed away from the surface.

1. RIDGE:

ID	Q*	G	H	LE	LE_{EQ}	α	β	T_A
0307	16.43	1.22	7.57	7.64	8.25	.926	.992	9.9
0407	17.17	1.41	7.57	8.18	8.94	.916	.926	12.1
0507	13.39	1.47	5.24	6.68	6.87	.973	.784	14.0
0707	12.50	1.50	3.66	7.34	6.56	1.120	.498	15.5
0807	6.37	0.66	1.82	3.88	3.78	1.033	.468	21.4
0907	13.58	1.29	4.69	7.60	7.60	1.000	.617	17.2
1007	7.33	0.98	1.53	4.82	4.27	1.129	.317	23.3
1507	11.98	0.93	4.78	6.27	6.43	.976	.761	14.1
2107	15.63	0.87	7.19	7.57	8.22	.921	.950	11.9
2207	12.96	1.00	3.87	7.99	7.26	1.101	.497	15.6
2707	12.18	0.90	5.35	5.93	6.41	.925	.903	12.5
2807	8.58	1.17	2.04	5.39	5.00	1.078	.378	21.3
Average	12.35	1.12	4.62	6.61	6.63	.997	.698	15.9

2. SWAMP:

ID	Q*	G	H	LE	LE_{EQ}	α	β	T_A
0307	19.28	1.34	6.50	11.45	8.96	1.278	.568	6.7
0407	16.84	1.10	4.99	10.76	8.37	1.286	.463	8.8
0507	13.77	1.38	3.18	9.20	6.93	1.327	.345	11.7
0707	13.98	1.29	3.27	9.43	7.45	1.267	.346	13.7
0807	6.54	0.38	1.31	4.85	4.00	1.212	.231	20.0
0907	15.57	1.40	3.22	11.05	8.65	1.277	.292	15.9
1007	8.76	0.78	1.30	6.68	5.33	1.254	.194	21.3
1507	13.73	1.13	3.94	8.66	6.73	1.286	.455	10.4
2107	17.22	1.59	5.33	10.31	8.18	1.260	.517	9.3
2207	18.34	1.87	4.21	12.26	9.67	1.269	.343	13.4
2707	13.80	1.18	3.50	9.12	6.88	1.326	.384	10.4
2807	10.46	1.03	1.61	7.82	6.27	1.247	.205	20.7
Average	14.04	1.21	3.53	9.30	7.28	1.277	.380	13.5

3. LAKE:

ID	Q*	G	H	LE	LE_{EQ}	α	β	T_A
0307	21.50	-2.28	7.84	15.94	12.93	1.233	.492	6.2
0407	22.54	9.55	3.98	9.01	7.12	1.266	.442	8.5
0507	19.02	0.96	4.34	13.72	10.99	1.249	.316	10.9
0707	19.81	14.14	1.08	4.59	3.45	1.331	.235	13.0
0807	8.68	1.55	1.22	5.91	4.64	1.273	.207	16.3
0907	19.22	7.35	2.67	9.20	7.41	1.242	.290	15.0
1007	10.08	1.67	0.64	7.77	5.66	1.373	.083	18.8
1607	17.02	-4.99	8.54	13.47	11.02	1.222	.634	5.9
2107	15.00	13.28	0.39	1.33	1.05	1.262	.294	11.8
2207	21.64	0.93	4.82	15.89	12.56	1.265	.303	13.3
2707	14.35	3.02	3.79	7.54	6.14	1.227	.503	9.7
2807	11.02	3.65	1.67	6.70	4.57	1.246	.294	16.0
Average	16.66	4.07	3.42	9.17	7.30	1.257	.372	12.8

APPENDIX E

DATA USED IN THE TEST OF THE RIDGE, SWAMP AND LAKE EVAPORATION MODELS

The following symbols are used:

LE_R = Evaporation estimates by the ridge model

LE_S = Evaporation estimates by the swamp model

LE_L = Evaporation estimates by the lake model

ID = Date (day-month-year)

LE = Measured evaporation

T_A = Average screen height air temperature (C)

K↓ = Incoming solar radiation

NH = Number of half-hours involved in the daily calculation

ND = Number of days involved in the monthly totals

For the ridge and swamp models the fluxes are in MJ m^{-2} day^{-1}. For the lake the fluxes are in 2MJ m^{-2} $week^{-1}$ and MJ m^{-2} mon^{-1}. Except for K↓, all fluxes are positive if directed away from the surface.

1. DATA USED IN THE TEST OF LE_R:

a. Pen Island 1971: (from Rouse and Stewart, 1972)

ID	NH	LE	T_A	K+	LE_R
060771	16	4.728	9.6	15.06	4.311
07	22	7.351	18.3	23.40	8.174
11	24	6.424	15.3	20.40	6.411
21	12	1.356	9.0	6.06	1.385
23	18	3.759	11.4	18.84	3.187
24	20	4.585	12.9	16.56	4.928
26	14	3.103	12.0	13.23	3.989
290771	22	7.353	13.0	23.68	7.484
030871	18	5.466	19.2	16.22	5.562
04	22	7.293	24.7	17.47	6.378
05	6	0.493	14.6	2.24	0.472
06	26	7.337	13.5	21.10	6.323
07	16	5.234	15.2	14.94	4.791
11	22	7.015	10.1	22.74	6.710
12	8	3.063	12.0	10.03	3.188
13	20	5.033	8.3	19.35	5.414
14	16	6.114	16.9	17.58	6.020
23	12	4.112	10.6	13.43	4.066
250871	22	4.824	14.1	16.96	5.072

1. DATA USED IN THE TEST OF LE_R:

b. Hawley Lake 1970: (from Rouse and Kershaw, 1971)

ID	NH	LE	T_A	K↓	LE_R
100770	22	6.183	16.4	19.73	6.416
18	12	2.765	14.4	9.67	2.945
19	28	7.115	12.8	23.73	7.090
20	16	5.933	17.9	17.62	6.150
24	16	6.159	23.7	15.76	5.959
27	16	4.475	15.0	17.06	5.601
28	16	6.034	13.7	19.32	6.319
290770	6	1.508	12.0	6.03	1.842

2. DATA USED IN THE TEST OF LE_S:

Thor Lake, N.W.T., 1974: (Measured by author)

ID	NH	LE	T_A	K↓	LE_R
300674	18	8.006	17.8	14.13	7.638
010774	25	7.528	15.5	14.39	7.144
02	21	3.436	12.1	8.43	3.640
03	25	5.703	14.0	12.84	6.071
04	25	8.630	15.5	18.16	9.313
05	25	8.453	16.2	16.44	8.437
06	25	9.612	16.6	18.15	9.506
07	25	8.158	16.0	16.10	8.207
08	25	8.143	17.5	15.33	7.983
10	22	7.170	16.1	14.40	7.371
110774	20	8.758	18.6	15.85	8.704

3. DATA USED IN THE TEST OF LE_L:

Perch Lake: 1970, 1971, 1972 (from Ferguson and Den Hertog, 1975)

a. 2-Weekly Totals:

ID	LE	T_A	K↓	LE_L
1906-020770	130.43	15.8	231.60	143.97
0907-1507	63.98	20.3	102.52	75.40
1607-2907	124.07	19.6	202.55	136.48
3007-1208	172.54	21.0	267.27	181.04
1308-2708	144.18	17.6	214.13	138.51
2808-1009	114.26	14.2	157.99	98.31
1109-240970	72.82	12.0	93.11	59.28
1606-290671	109.11	19.0	147.24	101.09
0808-2208	150.25	18.6	234.62	153.56
2208-0609	90.04	15.8	159.43	102.27
0609-2009	80.90	15.7	102.53	69.26
2109-041071	82.88	11.7	117.91	71.84
1306-260672	112.71	15.1	188.76	117.60
1107-2407	99.55	20.7	146.90	103.99
2507-0708	168.73	16.5	257.06	160.81
0808-200872	92.05	14.0	162.73	100.57

Perch Lake: 1970, 1971, 1972

b. Monthly Totals:

ID	ND	LE	T_A	K↓	LE_L
-0670	12	123.98	15.5	215.96	132.71
07	24	216.37	20.0	338.92	230.46
08	31	344.04	17.6	498.28	321.13
-0970	24	141.87	13.0	209.86	176.47
-0671	21	185.78	17.2	324.51	208.19
07	14	124.69	16.8	210.93	134.56
08	31	305.41	17.3	458.96	296.51
-0971	30	149.88	14.6	257.36	166.52
-0672	16	144.81	15.9	273.63	170.03
07	29	263.01	18.4	449.39	294.72
-0872	20	173.21	14.6	285.66	175.41

REFERENCES

Anderson, E.R., 1954: Energy-Budget Studies. In Water-Loss Investigations -- Lake Hefner Studies, Technical Report: *U.S. Geol. Survey Prof. Paper 269*, pp. 71-119.

Bowen, I.S., 1926: The Ratio of Heat Losses by Conduction and by Evaporation from Any Water Surface. *Phys. Rev.*, 27, pp. 779-789.

Cook, N.H. and E. Rabinowicz, 1963: *Physical Measurements and Analysis*. Reading, Mass.: Addison-Wesley Publ. Co., 312 pp.

Davies, J.A., 1967: A Note on the Relationship Between Net Radiation and Solar Radiation. *Quart. J. Roy. Met. Soc.*, 93, pp. 109-115.

Davies, J.A., 1972: Actual, Potential and Equilibrium Evaporation for a Bean Field in Southern Ontario. *Agr. Meteor.*, 10, pp. 331-348.

Davies, J.A. and C.D. Allen, 1972: Equilibrium, Potential and Actual Evaporation from Cropped Surfaces in Southern Ontario. *J. Appl. Meteor.*, 12, pp. 649-657.

Davies, J.A. and W.B. Schertzer, 1974: Canadian Radiation Measurements and Surface Radiation Balance Estimates for Lake Ontario During IFYGL. Final Report. IFYG. Proj. Nos. 71EB and 80EB, Dept. of Environment, Canada Centre for Inland Waters, Burlington, Ontario, pp. 77.

Denmead, O.T. and I.C. McIlroy, 1970: Measurements of Non-Potential Evaporation from Wheat. *Agr. Meteor.*, 7, pp. 285-302.

Dilley, A.C., 1968: On the Computer Calculations of Vapour Pressure and Specific Humidity Gradients from Psychrometric Data. *J. Appl. Meteor.*, 7, pp. 717-719.

Dyer, A.J., 1967: The Turbulent Transport of Heat and Water Vapour in an Unstable Atmosphere. *Quart. J. Roy. Met. Soc.*, 93, pp. 501-508.

Ferguson, H.L. and G. Den Hertog, 1975: Meteorological Studies of Evaporation at Perch Lake, Ontario. Unpublished Draft Report. Atmospheric Environment Service, Downsview, Ontario, pp. 12.

Fritschen, L.J., 1967: Net and Solar Radiation Relations Over Irrigated Field Crops. *Agr. Met.*, 4, pp. 55-62.

Fuchs, M. and C.B. Tanner, 1970: Error Analysis of Bowen Ratios Measured by Differential Psychrometry. *Agr. Meteor.*, 7, pp. 329-334.

Gay, L.W., 1971: The Regression of Net Radiation Upon Solar Radiation. *Arch. Met. Geoph. Biokl., Series B*, 19, pp. 1-14.

Goff, J.A. and S. Gratch, 1946: Low Pressure Properties of Water from -160 to 212 F. *Trans. Am. Soc. Heat. Vent. Eng.*, 52, pp. 95-121.

Harbeck, G.E., Jr., M.D. Kohler, G.E. Koberg, *et al.*, 1958: Water-Loss Investigations -- Lake Mead Studies. *U.S. Geol. Survey Paper 298*, pp. 100.

Idso, S.B., D.G. Baker and B.L. Blad, 1969: Relations of Radiation Fluxes Over Natural Surfaces. *Quart. J. Roy. Met. Soc.*, 95, 244-257.

Kershaw, K.A. and W.R. Rouse, 1973: Studies on Lichen Dominated Systems. I. The Water Relations of Cladonia Alpestris in Spruce-Lichen Woodland in Northern Ontario. *Can. J. Bot.*, 49, pp. 1389-1399.

King, K.M., 1961: Evaporation from Land Surfaces. *Proc. Hydrol. Symp. No. 2*, Nat. Res. Counc., Ottawa, pp. 55-80.

McNaughton, K.G. and T.A. Black, 1973: A Study of Evapotranspiration from a Douglas Fir Forest Using the Energy Balance Approach. *Water Res. Res.*, 9, pp. 1579-1590.

Monteith, J.L. and G. Szeicz, 1961: The Radiation Balance of Bare Soil and Vegetation. *Quart. J. Roy. Met. Soc.*, 87, pp. 159-170.

Monteith, J.L., 1965: Evaporation and Environment. *Symp. Soc. Expt. Biol.*, 19, pp. 205-234.

Nunez, M., J.A. Davies and P.J. Robinson, 1971: Solar Radiation and Albedo at a Lake Ontario Site. *Third Report.* Dept. of Geography, McMaster University, Hamilton, Ontario, pp. 82.

Penman, H.L., 1948: Natural Evaporation from Open Water, Bare Soil and Grass. *Proc. Roy. Soc. London, A. 193*, pp. 120-145.

Priestley, C.H.B. and R.J. Taylor, 1972: On the Assessment of Surface Heat Flux of Evaporation Using Large-Scale Parameters. *Mon. Wea. Rev.*, 100, pp. 81-92.

Robinson, P.J., J.A. Davies and M. Nunez, 1972: Longwave Radiation Exchanges Over Lake Ontario. *Fourth Report.* Dept. of Geography, McMaster University, Hamilton, Ontario. pp. 135.

Rouse, W.R. and K.A. Kershaw, 1971: The Effects of Burning on the Heat and Water Regimes of Lichen-Dominated Subarctic Surfaces. *Arctic and Alpine Res.*, 3, pp. 291-304.

Rouse, W.R. and R.B. Stewart, 1972: A Simple Model for Determining Evaporation for High-Latitude Upland Sites. *J. Appl. Meteor.*, 11, pp. 1063-1070.

Rouse, W.R., 1973: The Microclimatology of Different Terrain Units in the Hudson Bay Lowlands. *Proc.: Symp. on the Physical Environment of the Hudson Bay Lowland*, University of Guelph, Guelph, Ontario, pp. 69-82.

Rouse, W.R. and K.A. Kershaw, 1973: Studies on Lichen-Dominated Systems. VI. Interrelations of Vegetation and Soil Moisture in the Hudson Bay Lowlands. *Can. J. Bot.*, 51, pp. 1309-1316.

Shaw, R.H., 1956: A Comparison of Solar Radiation and Net Radiation. *Bull. Amer. Met. Soc.*, 37, pp. 205-206.

Slayter, R.O. and I.C. McIlroy, 1961: *Practical Microclimatology.* CSIRO, Melbourne, Australia, pp. 310.

Stewart, R.B., 1972: An Evaporation Model for High Latitude Upland Lichen Surfaces. Unpubl. M.Sc. Thesis, McMaster University, Hamilton, Ontario, pp. 47.

Swinbank, W.C., and A.J. Dyer, 1967: An Experimental Study in Micrometeorology. *Quart. J. Roy. Met. Soc.*, 93, pp. 494-500.

Tanner, C.B. and M. Fuchs, 1968: Evaporation from Unsaturated Surfaces: A Generalized Combination Method. *J. Geoph. Res.*, 73, pp. 1299-1304.

Thom, A.S., 1972: Momentum, Mass and Heat Exchange of Vegetation. *Quart. J. Roy. Met. Soc.*, 98, pp. 124-134.

Vries, D.A. de, 1963: Thermal Properties of Soils. In: *Physics of the Plant Environment.* North-Holland Publ. Co., Amsterdam, pp. 210-235.

Weaver, D.F., 1970: Radiation Regime Over Arctic Tundra and Lake, 1966. *Scientific Report.* Office Naval Res., Con. No. N00014-67-A-0007. pp. 31

Wilson, R.G., 1971: Evapotranspiration Estimates from the Water Balance and Equilibrium Models. Unpub. Ph.D. Thesis, Dept. of Geography, McMaster University, Hamilton, Ontario, pp. 123.

Wilson, R.G. and W.R. Rouse, 1972: Moisture and Temperature Limits of the Equilibrium Evapotranspiration Model. *J. Appl. Meteor.*, 11, pp. 436-442.